THE ROLE OF DIFFUSION WEIGHTED MAGNETIC RESONANCE IMAGING

AND APPARENT DIFFUSION COEFFICIENT QUANTIFICATION IN THE

EVALUATION OF PULMONARY LESIONS WHICH ARE INDETERMINATE

ON CONTRAST ENHANCED COMPUTED TOMOGRAPHY

A DISSERTATION SUBMITTED IN PARTIAL FULFILMENT OF THE M.D.

RADIODIAGNOSIS (BRANCH VIII) EXAMINATION OF THE TAMIL NADU

DR. M.G.R MEDICAL UNIVERSITY, CHENNAI TO BE HELD IN MAY, 2019.

CERTIFICATE

This is to certify that the dissertation entitled "The role of diffusion weighted magnetic resonance imaging and apparent diffusion coefficient quantification in the evaluation of pulmonary lesions which are indeterminate on contrast enhanced computed tomography" is the bonafide original work of Dr. Shweta Singh submitted in partial fulfilment of the requirement of the M.D. Radiodiagnosis (Branch VIII) Degree Examination of the Tamil Nadu Dr. M.G.R. Medical University, Chennai to be held in May 2019.

Guide:

Dr. Binita Riya Chacko

Professor,

Department of Radiology,

Christian Medical College,

Vellore.

CERTIFICATE

This is to certify that the dissertation entitled "The role of diffusion weighted magnetic resonance imaging and apparent diffusion coefficient quantification in the evaluation of pulmonary lesions which are indeterminate on contrast enhanced computed tomography" is the bonafide original work of Dr. Shweta Singh submitted in partial fulfilment of the requirement of the M.D. Radiodiagnosis (Branch VIII) Degree Examination of the Tamil Nadu Dr. M.G.R. Medical University, Chennai to be held in May 2019.

Dr. Sridhar Gibikote

Professor and Head

Department of Radiology

Christian Medical College

Vellore

CERTIFICATE

This is to certify that the dissertation entitled "The role of diffusion weighted magnetic resonance imaging and apparent diffusion coefficient quantification in the evaluation of pulmonary lesions which are indeterminate on contrast enhanced computed tomography" is the bonafide original work of Dr. Shweta Singh submitted in partial fulfilment of the requirement of the M.D. Radiodiagnosis (Branch VIII) Degree Examination of the Tamil Nadu Dr. M.G.R. Medical University, Chennai to be held in May 2019.

Dr. Anna B. Pulimood

Principal

Christian Medical College

Vellore

PLAGIARISM CHECK REPORT

[Urkund] 1% similarity - shweta4756@gmail.com Inbox ×

report@analysis.urkund.com   6:32 PM (10 minutes ago)
to me ▾

Document sent by: shweta4756@gmail.com
Document received: 10/9/2018 3:02:00 PM
Report generated 10/9/2018 3:02:58 PM by Urkund's system for automatic control.

Student message: Name: Dr. Shweta Singh
email ID: shweta4756@gmail.com
PG registration number (Tamil Nadu Dr. M.G.R Medical University):
201618056
Institute: Christian Medical College, Vellore

Document : Shweta-thesis-plagiarismCheck.docx [D42325720]

IMPORTANT! The analysis contains 1 warning(s).

About 1% of this document consists of text similar to text found in 70 sources. The largest marking is 38 words long and is 96% similar to its primary source.

PLEASE NOTE that the above figures do not automatically mean that there is plagiarism in the document. There may be good reasons as to why parts of a text also appear in other sources. For a reasonable suspicion of academic dishonesty to present itself, the analysis, possibly found sources and the original document need to be examined closely.

ACKNOWLEDGEMENTS

CONTENTS

INDEX OF TABLES AND FIGURES

ABSTRACT

Title:

The role of diffusion weighted magnetic resonance imaging and apparent diffusion

coefficient quantification in the evaluation of pulmonary lesions which are indeterminate on

contrast enhanced computed tomography.

Aims and objectives:

To assess the value of absolute signal intensity, lesion to spinal cord ratio (LSR) and apparent diffusion

coefficient (ADC) values obtained from the solid and necrotic components of indeterminate pulmonary

lesions in differentiating benign from malignant lesions.

Materials and methods:

Forty seven consecutive patients with indeterminate pulmonary lesions detected on contrast

enhanced CT of thorax who fulfilled the selection criteria for the study underwent MRI with

T2 weighted and diffusion weighted imaging (DWI) (b= 0, 500, 1000 s/mm^2). On DWI, the

absolute signal intensity, signal intensity of the lesion as compared subjectively to that of the

thoracic skeletal muscles (hypointense, isointense or hyperintense) and the LSRs (average of

3 values) were obtained following which ADC values of the solid and necrotic parts of the

lesion were assessed. The values for benign and malignant lesions and were compared using

the independent samples T- test. Receiver operating characteristic curves (ROC) were plotted

and diagnostic cut-off values were obtained.

Results:

Of the total of 47 patients enrolled (32 men; 15 women), 43 were diagnosed on histopathology

and the rest, on sputum culture or follow up after antibiotic therapy. On performing a qualitative

analysis comparing the signal intensity of the lesion on DWI (b=500 and 1000 s/mm^2) to that

of the thoracic skeletal muscle, most benign (N=27) and malignant lesions (N=20) were found

1

to be hyperintense on DWI with no statistically significant difference on b=500 s/mm^2 images (p value = 0.590) and b= 1000 s/mm^2 images (p value = 0.590). On comparing benign versus malignant lung lesions, statistically significant difference was seen between the absolute signal intensity of the solid component of the lesion on DWI (b=1000 s/mm^2) (p value =0.002; 95% CI 2.04 to 105.22), LSR on DWI (b=500 s/mm^2 (p value=0.002; 95% CI 0.24 to 0.97) and b= 1000 s/mm^2 (p value= 0.001; 95% CI 0.29 to 1.06)) and ADC of the solid component (p value= 0.006; 95% CI 0.079 to 0.969 x 10^{-3} mm$^{2/}$s). There was no statistically significant difference between absolute signal intensity values of benign and malignant lesions on b=500 s/mm^2 images (p value= 0.059; CI =105.22 to 2.04 x 10^{-3} s/mm^2).

For differentiation of malignant from benign lesions, ROC curves for LSR on DWI b=500 s/mm^2 yielded a cut-off value of 1.234 with 70.0% sensitivity and 74.1% specificity (AUC= 0.761), LSR on DWI b=1000 s/mm^2 yielded a cut-off value of 1.141 with 70% sensitivity and 85.2% specificity (AUC = 0.765) and ADC values of the solid component yielded a cut-off value of 1.248 x 10^{-3} mm^2/s with 80% sensitivity and 74.1% specificity (AUC= 0.735). Higher LSR values and lower ADC values are suggestive of malignancy. Some malignant lesions like mucinous adenocarcinoma (2/4) and squamous cell carcinoma (2/5) showed ADC values higher than the said cut-off value and a few cases benign lesions of tuberculosis (2/11), fungal infection (1/3) and a case of amyloidosis showed ADC values lower than that of the cut-off.

12 of 27 benign and 5 of 20 malignant lung lesions had areas of necrosis with no significant difference in the ADC of the necrotic components in the two groups (p value= 0.132; 95% CI 1.393 to 0.201 x 10^{-3} mm^2/s).

Conclusion:

DWI is a useful, safe, non-invasive tool for evaluation of pulmonary lesions which are indeterminate on CT. LSR and ADC of solid component are useful for differentiating bening

from malignant lesions with no significant difference in diagnostic performance between the them (p value= 0.779). If a lesion tests positive for malignancy for either of the tests, the overall sensitivity can be increased up to 94% (specificity = 63.1%). In patients with high risk for lung biopsy, DWI & ADC maps in addition to CECT, can further assess the likelihood of malignancy and help direct further management.

Keywords: diffusion weighted magnetic resonance imaging, b factor, absolute signal intensity, lesion to spinal cord ratio, apparent diffusion coefficient, indeterminate pulmonary lesions

INTRODUCTION

With the advent of computed tomography (CT), there has been an increase in the number of pulmonary lesions detected in patients undergoing CT of thorax for related or unrelated reasons. In a patient detected to have a pulmonary lesion, it is vital to arrive at a diagnosis which would direct further management. CT of the thorax with contrast (CECT) has significantly improved the ability to localize and characterize pulmonary lesions over plain chest radiograph (1). It is often possible to arrive at a single diagnosis based on CT findings and the clinical presentation of the patient. However, in some cases, it may not be possible to further characterize the lesions and differential diagnosis could include infectious, inflammatory causes and malignancy.

Lung lesions can be categorised on CT in to nodule, mass, cavity, consolidation and ground glass opacity. Both malignancy and infection can present as nodule, mass like lesion, cavity, consolidation and ground glass opacity. Most infectious and inflammatory lesions can be empirically treated based on imaging findings with corroborative clinical features and lab investigations. However, obtaining a tissue diagnosis is vital prior to initiating treatment of malignancy, for definitive diagnosis, obtaining the histopathological subtype, immunohistochemistry and genetic studies that direct surgery, chemotherapy and radiotherapy. Lung carcinoma is still one of the leading causes of cancer related death and early diagnosis is so important that developed countries have established screening methods for at-risk population.

Diffusion weighted imaging (DWI) which has shown promising results in differentiating malignant from benign lesions in the brain and prostate is now being explored for its possible use in evaluating pulmonary lesions. There have been a few studies in the recent past which have looked at differences in DWI and ADC in biopsy proven benign and malignant lesions with promising results. On review of literature, we found no dedicated studies assessing the additional role of DWI to evaluate pulmonary lesions which cannot be diagnosed on CT as probably malignant or probably benign. When CT findings are equivocal, the use of advanced imaging help identify the cases where the risk to benefit ratio of performing lung biopsy is great.

The purpose of this prospective study is to additionally characterize pulmonary lesions which are indeterminate on CT, using visual and quantitative analysis of DWI and ADC maps and reveal its role in contributing to diagnosis of malignancy versus infection. The final diagnoses in our patients were based on biopsy and histopathological examination, clinical follow up and other corroborative investigations.

AIMS AND OBJECTIVES

Aim:

To assess the role of diffusion weighted magnetic resonance imaging and apparent diffusion coefficient quantification in the evaluation of pulmonary lesions which are indeterminate on contrast enhanced CT of the thorax.

Primary objectives:

1. To assess the average ADC values from the solid component of the lesions and assess difference in ADC values between malignant and benign lesions.
2. To obtain the absolute signal intensity of pulmonary lesions on DWI b=500 s/mm^2 and b=1000 s/mm^2 images and assess the difference in absolute signal intensity between malignant and benign lesions.
3. To obtain the lesion to spinal cord signal intensity ratio (LSR) and assess difference in LSR between malignant and benign lesions.
4. To grade the signal intensity of pulmonary lesions on DWI images in comparison to the thoracic skeletal muscle and assess difference between that of malignant and benign lesions.

Secondary objectives:

1. To assess the difference in ADC values obtained from necrotic areas within benign and malignant lesions.

REVIEW OF LITERATURE

In a patient detected to have a pulmonary lesion, it is vital to arrive at a diagnosis which would help direct further management, be it conservative follow up or aggressive medical or surgical treatment (1). Lung lesions can be categorised on CT in to consolidation, cavity, nodule, mass, and ground glass opacity. Malignancy, infection and inflammatory causes can have these appearances on CT.

Consolidation

Consolidation is a term used to describe filling of airspaces in the pulmonary tree with a material which increases its relative attenuation with that of the surrounding normal lung parenchyma (2). A consolidation is an area of increased lung parenchymal attenuation with obscuration of the pulmonary vessels (sometimes with an air bronchogram) without any significant volume loss of the affected segment. A ground glass opacity is defined as increased lung parenchymal attenuation without obscuration of the pulmonary vessels. The increase in parenchymal attenuation may occur due to filling of air-spaces with fluid (pulmonary edema), pus cells or other inflammatory cells (pneumonia), blood (haemorrhage), protein (alveolar proteinosis) or malignant cells (bronchoalveolar carcinoma). The distribution may be patchy (incomplete airspace filling with incontiguous areas of residual gas within alveoli), lobar (homogenous increase in attenuation of a lobe with clear delineation of adjacent normal lung) or multifocal. Definitive etiological diagnosis is determined by clinical presentation, microbiological and or histopathological correlation.

Based on the pattern of involvement, the causes can be classified as

1. Lobar

   a. Infectious - bacterial pneumonia

      b. Malignant - lung carcinoma with obstructive atelectasis or pneumonia, adenocarcinoma with endobronchial spread

      c. Vascular - contusion, infarction

      d. Others - organizing pneumonia, eosinophilic pneumonia, sarcoidosis

2. Diffuse

      a. Edema – pulmonary edema (cardiogenic, renal), acute respiratory distress syndrome (ARDS), hypoalbuminemia

      b. Infection – Viral, Pneumocystis jiroveci, staphylococcal bronchopneumonia

      c. Haemorrhage- Wegener's granulomatosis, Henoch Schonlein purpura (HSP), systemic lupus erythematosis (SLE)

      d. Others – Acute hypersensitivity pneumonitis, pulmonary alveolar proteinosis etc.,

3. Multifocal

      a. Bronchopneumonia (Klebsiella, Staphylococcus, Legionella, Gram negative bacteria, tuberculosis)

      b. Vascular – septic emboli, Wegener's granulomatosis

      c. Neoplasms- adenocarcinoma with endobronchial spread, lymphoma.

      d. Others- organizing pneumonia, eosinophilic pneumonia, lipophilic pneumonia

Definitive etiological diagnosis is determined by clinical presentation, microbiological and or histopathological correlation. There are however, some radiological features that could point to the diagnosis in certain cases. Common radiological signs associated with infection include the air bronchogram sign, the tree in bud sign associated with endobronchial spread of

infection (bacterial, mycobacterial, fungal etc), the bulging fissure sign associated with

Klebsiella pneumonia, air-fluid sign which may indicate an abscess within and the split

pleural sign which indicates as associated empyema. The feeding vessel sign is suggestive of

septic emboli, but can also be present in pulmonary metastases (3).

Cavity

Pulmonary cavities are air-filled space within a consolidation, mass or nodule and may be

seen both on plain chest radiographs or CT. The causes of pulmonary cavities are as follows-

- Infection
  - pulmonary tuberculosis
  - pulmonary bacterial abscess/cavitating pneumonia
  - septic pulmonary emboli
    - other rare infections (coccidioidomycosis, actinomycosis, nocardiosis , melioidosis, cryptococcosis)
- Cavitating malignancy
  - primary bronchogenic carcinoma (especially squamous cell carcinoma)
  - cavitating pulmonary metastases (squamous cell carcinoma, adenocarcinoma, sarcoma, tumours of the gastrointestinal tract and breast)

- Non-infective granuloma
  - rheumatoid nodules
  - granulomatosis with polyangitis
- Vascular
  - pulmonary infarct

These lesions are typically thick walled (2-5mm). A study done by Honda et al (2007) showed that presence of a notch in a cavitatory nodule and irregular internal wall was more commonly associated with malignancy while the presence of satellite nodule, linear margins, associated bronchial wall thickening and surrounding ground glass attenuation were more commonly associated with benign nodules (4). Post contrast enhancement, on the other hand can be seen in the walls of both infectious and malignant cavitatory lesions.

Nodule:

Pulmonary nodules are solitary or multiple focal, radiographic opacities. A classic solitary pulmonary nodule (SPN) is defined as a single, spherical, well-circumscribed, radiographic opacity measuring less than or equal to 30 mm in diameter and is surrounded completely by aerated lung. Pulmonary nodules may be solid or sub-solid. The latter group is further subdivided into part- solid and pure ground glass nodule. A solid nodule is an air-space opacification with higher density than the surrounding parenchyma which may obscure underlying bronchovascular structures while a ground glass nodule is an ill-defined area of high attenuation which does not obscure bronchovascular structure. Solid pulmonary nodules could represent various etiologies like-

- Benign granulomas
- Intrapulmonary lymph node
- Focal scar
- Primary lung malignancy
- Pulmonary metastases

These nodules have considerable overlap in their radiological features and follow up based on size recommended by the Fleischner's guidelines.
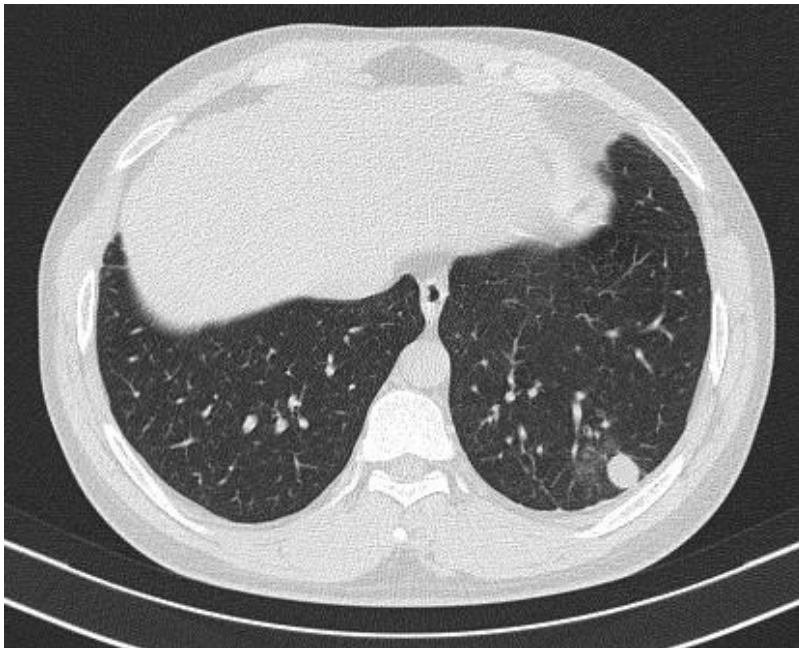
Figure 1: Interstitial pneumonia with eosinophilic granulomas presenting as a solid left lower lobe pulmonary nodule in a patient.

Subsolid nodules (especially ground glass nodules) are often transient and are caused by haemorrhage or infection. However, persistent subsolid nodules could be representative of malignancy of the adenocarcinoma spectrum.

A solitary pulmonary nodule has been described by Erasmus et al as a 'discrete, well-circumscribed, rounded opacity less than or equal to 3 cm in diameter that is completely surrounded by lung parenchyma, does not touch the hilum or mediastinum, and is not associated with adenopathy, atelectasis, or pleural effusion' . This is often an incidental finding on chest radiographs/ contrast enhanced CT. In most cases, a benign etiology, commonly infection, is considered most likely. However, the challenge lies in differentiating these lesions from early stage lung cancer in a non-invasively and cost-effectively as is possible.(5)

Shi et al (6) studied the relationship between the size of a SPN and the chance of malignancy in a cohort at high risk for lung cancer and found that nodules <4mm) were least likely to be malignant. Central, popcorn like and laminated calcifications are likely to be of benign etiology. In a study by Henschke et al (7), part-solid nodules were malignant in 63% of part-solid nodules, 18 % of pure ground glass nodules and 7 % of solid nodules were found to be malignant. Presence of intranodular fat is indicative of a hamartoma. On the other hand, margins that are spiculated / irregular and distortion or encasement of adjacent bronchovascular structures are more commonly associated with malignancy(8). Post contrast enhancement of less than 15 HU is in favour of a benign lesion. A large number of lesion detected on CT, however, do not show features characteristic of either are and termed indeterminate. Thus there still remains a grey area of overlap in some lesional characteristics like attenuation values, presence of cavitation/ central necrosis and wall thickness among infectious and malignant lesions. Also, lesions like active granulomas and hypervascular benign tumors may show significant post contrast enhancement. In such cases PET-CT, MRI are other investigative modalities used for further characterization of the lesions as benign or malignant (9).

PET-CT, although known for its high sensitivity (95 %) has a low specificity (~81%) and granulomatous lesions (10) like those due to pulmonary tuberculosis may show false positive results, which is problematic in a country like India, which has a high prevalence of the disease .

Consolidating the various studies evaluating pulmonary nodules, the Fleischner society has drawn up guidelines for the management of solitary pulmonary nodules, updated in 2017 (11). This encompasses the professional opinions of an international consortium of pulmonologists, surgeons, pathologists and thoracic radiologists with new data and accumulated experiences.

Due to the overlapping features of benign and malignant pulmonary lesions manifesting as nodules, cavities, consolidations or masses on CECT, there is a need to use other imaging modalities and techniques, to differentiate between the two due to implications related to their management (including further imaging, need for biopsy and histopathological examination of these lesions which would direct treatment).

Pulmonary infections

Pulmonary infections are common pulmonary pathology. The appearance of these infections on CECT depend on the causative organisms, their mode of spread and the immune status of the host among other factors. These infections can spread through the tracheobronchial tree (through inhalation), via the pulmonary vessels (haematogeneously) or through continuous spread from adjacent structures.

Bacterial infections

Several virulent bacterial infections like that of *Streptococcus pneumonia, Klebsiella sp., Haemophilis influenzae* often manifest as lobar pneumonia. It often affects patients at extremes of ages, presenting as fever, productive cough and dyspnoea. Fibrosuppurative infiltrates fill the alveolar airspaces result in consolidation which imparts a homogeneous opacification of the lung tissue with no volume loss (which correspond to the pathological stages of red and grey hepatisation) on CT restricted to one or more lobes with and air-bronchogram and sometimes, with a syn-pneumonic effusion(12).

Tuberculosis

The imaging features of pulmonary tuberculosis (caused by *Mycobacterium tuberculosis*) vary depending on the host and whether it is a case of primary or post-primary tuberculosis. Patient often have low-grade or chronic symptoms and its radiological appearances are so varied that it sometimes results in diagnostic confusion it sputum examination does not yield the acid-fast bacilli.

In those with primary pulmonary TB, in an immunocompetent patient, the initial caseating granuloma, calcified forming a Ghon's focus (often peripherally located in the upper lobe or apical segment of the lower lobe), and may be associated with pleural effusion (commoner in adults). If, accompanied by mediastinal or hilar lymphadepathy, it is called a Ranke complex (which may be calcified in upto 35% of cases).

Post-primary TB is a result of reactivation and more commonly manifests as cavitations (20-45% of cases) and commonly involve the upper lobes (85%). The cavity may erode a nearby bronchus resulting in and air-fluid level within. Endobronchial spread results in a 'tree-in bud' appearance (branching peribronchial thickening with fine nodules) on HRCT and may be associated with hilar adenopathy.

Miliary tuberculosis, which results from haematogeneous dissemination of the bacillus, appears on CT as 1-3 mm nodules of uniform size and distribution.

In patients with co-existing HIV infection, which CD4 counts are between 350 and 200 cells/ mm^3 the manifestations resemble that of post-primary tuberculosis while in those with counts below 200 cells/ mm^3, military TB is more common with generalized lymphadenopathy (13)

Atypical mycobacterial infections

Other mycobacterial pulmonary infections, of which Mycobacterium avium-intracellulare is the most common, pulmonary manifestation seen on CT include ground-glass opacities, 'tree-in bud' appearance associated with endobronchial spread, areas of patchy consolidation and bronchiectasis with bronchial wall thickening ('tram-track sign') and pleural thickening. These lesions tend to have a predilection for the upper lobe, right middle lobe and lingual (14).

Fungal infections

These are commonly seen in immunocompromized patients who are diabetic, on long term steroid therapy, immunosuppressants or chemotherapy and those with HIV infection with low CD4 counts. Etiological agents include molds like *Aspergillus sp.* (most common), yeasts like *Candida sp.,* and dimorphic fungi like *Histoplasma capsulatum, Coccidoides immitis, Blastomyces sp.* etc. Pulmonary aspergillosis has varied radiological manifestations that depend largely on the immune response of the host.

Allergic bronchopulmonary aspergillosis is a result of a hypersensitivity reaction to the same and commonly manifests on CT as transient pulmonary alveolar ground glass opacities or centrilobular nodules and mucus plugging resulting in the typical 'finger-in glove' appearance. Over a long period of time, it can result in bronchiectasis and scarring.

Aspergillomas occur in immunocompetent patients with structurally abnormal lungs (i.e bronchiectasis, cavitation). It is a fungal ball formed by a mixture of fungal hyphae, reactive cellular debris and mucus within a cavity, with vascular granulation tissue within the walls (which results in haemoptysis). On CT this appears as a central rounded mass of soft tissue attenuation within a cavity, surrounded by an air-crescent (Monod sign) with mobility demonstrated on positional change.

Invasive aspergillosis is typically seen in immunocompromised host and may result in broncho-invasive or angio-invasive disease. Radiologically, broncho-invasive disease manifests as obstructive tracheobronchitis (characterized by bronchial wall thickening), bronchiolitis (imparting a 'tree in bud appearance') or bronchopneumonia (seen as peribronchial areas of patchy consolidation). Angio-invasive disease, seen in profoundly immunosuppressed patients, particularly in the setting of neutropenia (<500cell/mcL) post bone marrow transplant, typically manifests on HRCT as a nodule surrounded by ground glass opacitiy (which represents haemorrhage), known as the 'halo-sign' (12).

Pneumocystis pneumonia

The organism is a yeast-like atypical fungus that almost exclusively affecting immunocompromised hosts, especially HIV positive patients with a 200 cells/ mm^3. HRCT of the thorax shows predominantly perihilar pulmonary ground-glass opacities with a 'crazy paving' pattern of involvement with pneumatocoeles

Viral infections

These are causes by a host of RNA and DNA viruses, including the influenza viruses, the manifestations of which vary depending on the viral strain and host factors. On CT, the most common findings are bilateral peribronchial thickening in the perihilar regions with interstitial infiltrates and areas of patchy atelectasis and air-trapping(15).

Non-infectious inflammatory lung disease

This is a group of benign inflammatory pulmonary conditions which encompasses airspace predominant, vascular predominant and interstitial predominant disease. The air-space predominant lesions and some combined air-space/ interstitial disease like sarcoidosis often mimic infectious and malignant pulmonary lesions on CECT or HRCT (16).

Airspace predominant inflammatory lung disease

Eosinophilic pneumonias, especially the chronic subtype, is seen in the setting of asthma or a hypersensitivity response to certain drugs or part of fungal infections. CT shows areas of non-segmental peripherally located air-space consolidations and band like opacities parallel to the pleura which may later progress to fibrosis.

Organizing pneumonia is a non-specific response to pulmonary injury. The more common radiological appearance on CT is that of peripheral bilateral lower lobe predominant consolidations with air bronchograms and subpleural sparing and the 'atoll sign' which is an area of ground glass opacity surrounded by a rim of consolidation is typically described in this condition. However, occasionally, it may present as multiple lung masses that are PET avid and mimic carcinoma, leading to diagnostic confusion in such cases. Most of these case often resolve without specific treatment.

Langerhan cell histiocytosis and respiratory bronchiolitis associated interstitial lung disease are both associated with smoking (which is also associated with higher risk of malignancy). The conditions themselves, however, are benign and the patterns of involvement are in the form of micronodules, cystic or cavitatory lesions in LCH which responds to smoking cessation and centrilobular nodules (with or without emphysematous changes) in case of RB-ILD.

Vasculitis

This encompasses a group of inflammatory disorders mainly affecting the blood vessels of the lung and are often associated with systemic vasculitis. Among other subtypes mentioned in the Chapel Hill classification, they have varied appearances. In ANCA associated vasculitis, pulmonary nodules and areas of consolidation with cavitation are common and may be accompanied by mediastinal or hilar adenopathy and pleural effusion while on the other hand, Churg-Strauss syndrome presents with transient nodule, ground-glass opacities or patchy areas of mosaic attenuation and inter-lobular septal thickening with no specific lobar predilection. These appearances, however, may not be diagnostic. Thus, the clinical presentation, serum markers and imaging findings together help reach a diagnosis in most cases (17).

Sarcoidosis

It is a benign inflammatory systemic disorder characterized by noncaseating granulomatous disease. Pulmonary and mediastinal involvement in seen in up to ~90% of cases of sarcoidosis. CT features include ground glass opacities, interlobular septal thickening with centilobular nodules, confluence of smaller nodules that may mimic a consolidation often with enlarged mediastinal and hilar lymph nodes and in later stages, honeycombing and tractional bronchiectasis. Nodular sarcoidosis, in particular, often resembles primary or metastatic lung cancer on CT and is avid on PET. Differentiating it from lung carcinoma is important as it heralds a good prognosis and responds well to corticosteroid therapy(18).

Lung carcinoma

Epidemiology

Lung carcinoma is one of the most common causes of cancer related deaths, worldwide, in the last few decades and the global burden of disease study done in 2020 estimates that the economic burden of healthcare related costs for lung cancer and substantial (19). The incidence of lung cancer is 1.8 million (as of 2012) and is the responsible for 1.6 million cancer-related deaths that occur annually. It has a much lower five-year survival rate of 17.8% than most other causes of cancer (20).

In India, alone, it constitutes 6.9% of newly detected cases of cancer and 9.3% of deaths related to cancer, especially among males, with a rising trend among females. The disease also occurs more commonly in the elderly, with more than 70% of death occurring after the age of 65. The highest incidence is reported in the state of Mizoram (females and males) at age adjusted rates of 28.3 per 100,000 males and 28.7 per 100,000 females. The incidence of lung cancer has also risen in Metropolitan cities like Chennai, Bengaluru and Delhi (21). Although lung cancer is strongly associated with smoking, there is an increasing incidence of non-smokers who are affected by the disease. Adenocarcinoma is the most common histological type among these patients who, more often, are females and in some Asian populations, constitute up to ~25% of the patients with lung cancer (22). The high incidence of pulmonary tuberculosis in India further increases the risk of lung cancer in the affected population due to the parenchymal scarring which occurs as a sequel to previous infection (23).

Histopathology

The histopathological types of lung cancer are broadly divided into small cell lung cancer (SCLC) and non-small cell lung cancer (NSCLC) which includes adenocarcinoma, squamous cell and large cell carcinoma. Squamous cell carcinoma is most strongly associated with

cigarette smoking. There has been a rising incidence of adenocarcinoma in the last few decades which has now overtaken squamous cell carcinoma as the most common type.

With rapid improvements in molecular techniques, it is now of increasing importance to identify specific genetic mutations associated with the different types of lung carcinoma. Epidermal growth factor is a protein that stimulates tyrosine kinase. Up to 15% of patients in the USA have tested positive for epidermal growth factor receptor (EGFR) mutations. Overexpression of this receptor due to mutations in the tyrosine kinase domain of the EGFR gene, leads to increase tumour growth. This mutation is most often seen in non-smoking females with adenocarcinoma. In these patients treatment with targeted therapy using monoclononal antibodies like erlotinib can increase the response rate up to 70%.

Other mutations of genes encoding K-Ras protein, anaplastic lymphoma kinase (ALK) have also been studied to develop targeted therapy for patients with these mutations.

Environmental risk factors for lung carcinoma

Smoking

It is the most strongly associated risk factor which increases proportionately with the dose as confirmed in the landmark study by Doll and Hill (24). The tar and other components are carcinogenic which nicotine can promotes tumour growth.. It has been found that cessation of smoking decreases lung cancer risk (especially squamous cell and small cell carcinoma) which drops by 50% after a period of 15 years post cessation (25).

Pollutants and other carcinogens

Air pollutants are a proven risk factor for lung cancer. Particles of size less than 2.3micron are more strongly associated with increased risk of lung cancer. Among the materials

associated with occupational lung disease, asbestos exposure (especially to chrysolite fibres) is a known risk factor for both lung and pleural carcinoma (26).

Influence of cell-type on radiological appearance of lung carcinoma

Up to 2% lung tumours can have varied cellular composition (27) and multiple synchronous primary lung tumours of various histopathological types can co-exist (28). Despite these discrepancies, certain radiological appearances suggest certain histological types of lung carcinoma.

Adenocarcinoma

This tumour most commonly presents as a peripherally located solitary pulmonary mass and is often associated with large hilar lymphadenopathy. Some of these masses, at the time of diagnosis, may show evidence of mediastinal involvement.
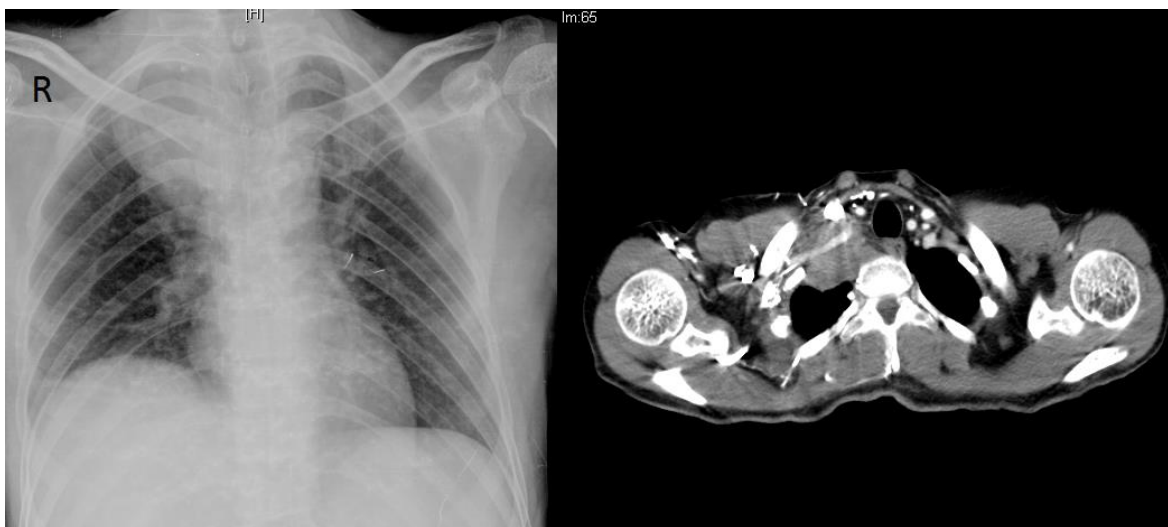
Figure 2: Superior Sulcus Tumor

It may present as a superior sulcus tumour, also known as a Pancoast tumour. This variety often invades the adjacent visceral and parietal pleura and the chest wall. Horner's syndrome (ptosis, miosis, enophthalmos and loss of ciliospinal reflex) with neck, shoulder pain and wasting of the lumbrical muscles is secondary to invasion of the superior cervical sympathetic ganglion and lower roots of the brachial plexus, respectively.
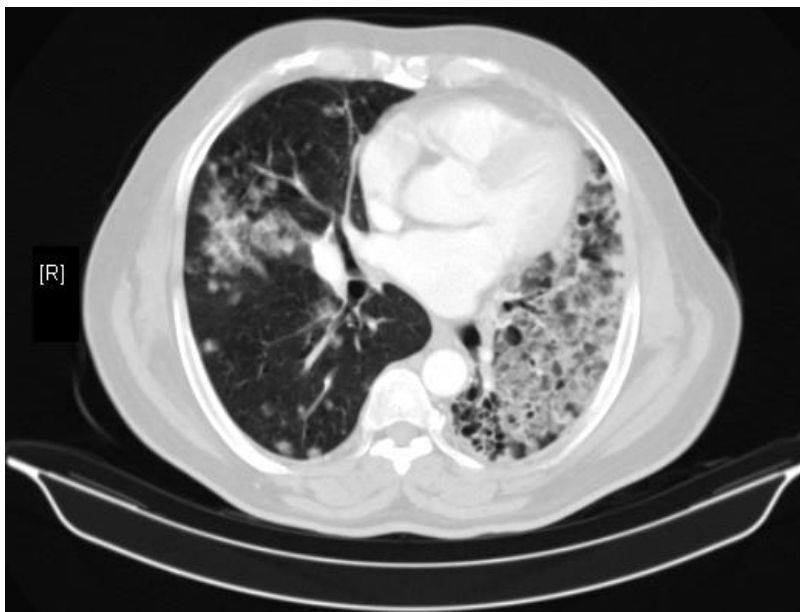
Figure 3: Consolidation in adenocarcinoma in situ

Adenocarcinoma in situ, formerly known as bronchoalveolar carcinoma, can show varied radiological appearances. It may present as a solitary pulmonary nodule in up to 43 %, consolidation or multicentric disease. Its presentation as diffuse consolidation can be explained by its unique pattern of growth, as it uses the alveoli as scaffolding stroma upon which it can grow and spread. Certain types of adenocarcinoma metastases (from primary tumours like the colon, pancreas and biliary tree) also may have a similar appearance. Desmoplastic reaction may lead to a spiculated margin and pleural tags. Pseudo-cavitation is

another described appearance (29) characterized by a peripheral heterogeneously enhancing lung mass with central areas of lucency and irregular margins forming a star-like pattern.
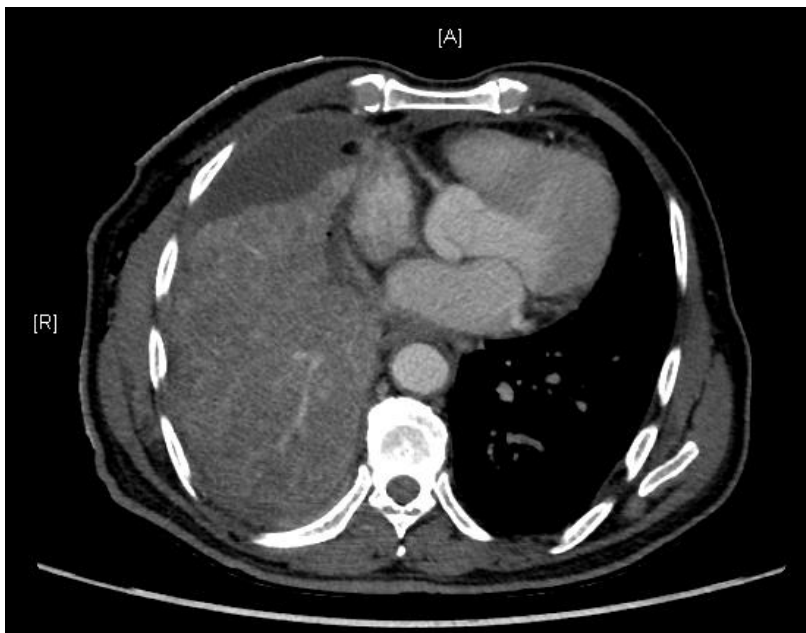
Figure 4: "CT angiogram sign"

Figure 5: "Cheerios in the chest"- cavitatory pulmonary lesions

Another radiological appearance on CT commonly associated with adenocarcinoma in situ or minimally invasive adenocarcinoma, is the "CT angiogram sign". The pulmonary vasculature

appears prominent against the background of consolidated lung with relatively lower attenuation. Other differential diagnoses for this radiological sign include pulmonary lymphoma and post-obstructive pneumonia (30)

Other radiological presentations include

- Atelectasis

- Expansile areas of consolidation without an air bronchogram

- Multifocal cavitatory lesions (cheerios sign) which is unusual in adenocarcinoma in situ due to lower propensity to outstrip its blood supply and undergo necrosis and its tendency to preserve the pulmonary architecture (31).

Squamous cell carcinoma (SCC)

These tumours are most commonly central in location. They may originate from the epithelial lining of the main or lobar or segmental bronchi. They form proliferative growths which result in bronchial obstruction and subsequently erode the bronchial walls.

Intraluminal tumours cause bronchial obstruction and post-obstructive collapse of the respective lobes. The resultant volume loss results in ipsilateral mediastinal shift and hemidiaphragmatic elevation with a juxta-phrenic peak (specifically, in cases associated with upper lobe collapse). This radiographic appearance was first described by Golden as seen on frontal chest radiographs. Collapse of the right upper lobe results in the same appearing dense and shifted centrally and upward with a centrally located mass causing expansion of the hilum. These two changes result in the formation of the reverse S-shape called the Golden S sign (32). Post-obstructive infective consolidation, on the other hand, differs in that there is relative preservation of volume.

Squamous cell carcinoma and adenocarcinoma can be associated with scar tissue occurring as a result of previous tuberculosis and other conditions. Enlargement of the scar on follow up images must raise the suspicion of carcinoma at the site of the scar (31).

SCC can invade the surrounding structures in the mediastinum including the aerodigestive tract and encase the great vessels. These tumours also metastasize frequently to the bone, liver and adrenal glands by hematogenous spread.

Small cell carcinoma

These are highly malignant neuroendocrine tumours which metastasize early in the course of the disease, hence harbour a relatively poorer prognosis. Most tumours are centrally located and associated with mediastinal lymphadenopathy. Less commonly, they may present as a peripherally located solitary pulmonary nodule, which carries a better prognosis.
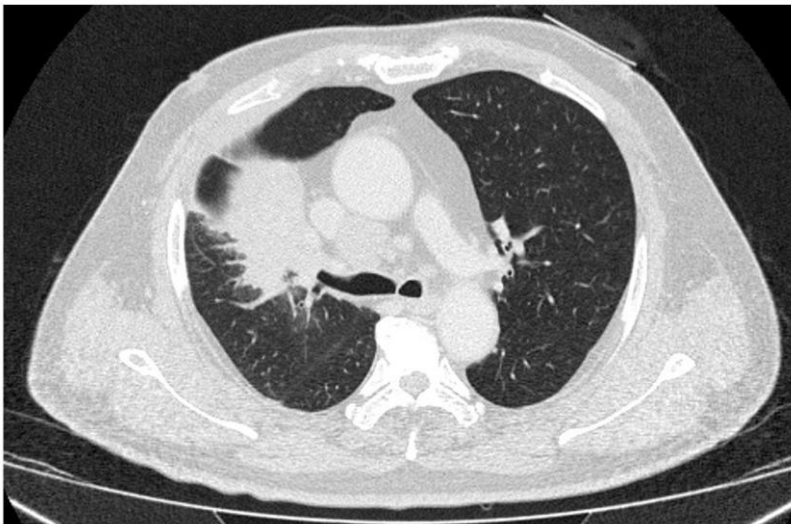
Figure 6: Small cell carcinoma of the right upper lobe with ipsilateral mediastinal lymphadenopathy (33)

Large cell undifferentiated carcinoma

These constitute nearly 10% of the cases of lung cancer. Histopathologically, they lack squamous, glandular or small-cell differentiation. These tumours grow rapidly, are large in size, often, peripherally located and associated with necrosis. They can potentially invade the pleura resulting in malignant pleural effusion and metastasize early.

Bronchial carcinoid

Bronchial carcinoid tumours are neuroendocrine lung tumours which originate in the bronchial or bronchiolar epithelium. They are typically endobronchial nodules or hilar or perihilar masses causing bronchial obstruction and post-obstructive collapse or consolidation. They show marked arterial phase enhancement due to rich vascular supply and may present with carcinoid syndrome due to secretion of various peptide hormones and neuroamines. (34). The peripheral, type, however, is a rare presentation, more commonly associated with smoking, that presents as a 10-30mm solitary pulmonary nodule with non-specific imaging features and are more often not associated with carcinoid syndrome. Although most cases are 18 FDG-PET avid, up to a fourth of these lesions may not show increased uptake(35).

Pulmonary lymphoma

Pulmonary lymphoma is lung parenchymal lymphomatous involvement. It may be primary or secondary. Primary pulmonary lymphoma is rare and often a type a non-Hodgkin lymphoma. It presents as a pulmonary mass or mass-like consolidation with or without lymphadenopathy which may be associated with pleural effusion. Secondary pulmonary lymphomas are more common and represent secondary involvement of the lung in a case of Hodgkin or Non-Hodgkin lymphoma. Pulmonary lymphoma may also present in the post-transplant setting or in patients with AIDS(36).

Screening for lung cancer

Chest radiograph

It is the earliest tool used for lung cancer screening. Although cost-effective and readily available at most centres, it is limited by its lower sensitivity and specificity. A few trials, carried out in Japan studied the use of chest radiographs as a screening tool and concluded that, in conjunction with sputum cytology, it conferred some advantage in early cancer detection and 5-year survival rates over no screening, but with no overall advantage for long term (20 year) survival (37),(38).

CT screening

With the advent of low-dose techniques, the use of CT in screening for lung cancer has been extensively studies. These studies looked at high-risk populations. The first few studies performed in Japan (39). In these studies, follow up of detected nodules was based on size (large nodule were subject to biopsy/ FNAC, nodule of intermediate size were screened at defined intervals and very small nodules were not followed up). This, along with later studies like Henschke et al's "Early Lung Cancer Action Project" (7) showed that lung cancer diagnosed at earlier stage using CT for screening had better treatment response and prognosis that those detected at later stages.

With earlier CT image acquisition techniques, the accuracy was limited. However, with improving technology, namely multi-detector CT (which can produce 1mm contiguous sections) and reconstruction techniques like maximum intensity projection, there has been improved conspicuity of pulmonary nodules. Computer-aided Diagnosis (CAD) improves the

radiologist's detection of nodules, while allowing the latter to use his/her discretion to deem them as clinically significant. Whatever be the technique, radiologists, world over use standard diagnostic and reporting guidelines like those laid out by the Fleischner Society.

Diffusion weighted imaging

Diffusion weighted imaging is a technique in MRI that is based on differential Brownian motion of water molecules in various tissue and helps evaluation the micro-architecture of these tissues. Intracellular water molecules have greater diffusion restriction than free water. Thus depending on the tissue architecture, degree of cellularity and the varying proportions of intracellular and extracellular compartments, the degree of diffusion restriction also varies between tissues and also between pathological areas within the a tissue against its normal background . Certain high grade malignancies and tissues that have undergone acute infarction show diffusion restriction due to the increased proportion of intracellular to extracellular water molecules. Diffusion weighted imaging thus helps qualitatively and quantitatively identify and measure diffusion restriction.

The advent of magnetic resonance imaging in modern clinical medicine in the 1970s is credited to Lauterbur, Ernst R and Mansfield (40) Diffusion weighted imaging (DWI) was the result of research efforts of doctors like Tanner, Stejskal and Le Bihan who tried to differentiate malignant liver tumours from angiomas (41). Susceptibility to respiratory motion artefacts were, however, a major limitation. With the advent of echo-planar imaging and higher magnetic field strengths (1.5T, 3T) clinically useful diffusion weighted imaging of the abdomen and thorax became a reality due to shorter imaging time and increased signal to noise ratio.

In order to obtain a DWI sequence, a diffusion sensitization gradient is applied on both sides of the 180 degree refocussing pulse. The 'b value' a measure of the degree of applied diffusion weighting. It is represented by the following equation –

$b = \gamma^2 \, G^2 \, \delta^2 \, (\Delta - \delta/3)$

G = amplitude

δ = time of applied gradients

Δ = duration between paired gradients

Therefore, larger 'b values' may be obtained by widening the time interval between paired gradient pulses and increasing the duration and gradient amplitude.

Therefore, to detect smaller lesions and slower moving water molecules within their intracellular compartments, a higher 'b value' is considered more suitable (i.e. b= 500 to 1000 s/mm^2). ADC values are calculated using a dedicated software and a parametric map generated which reflects the degree of diffusion restriction by drawing regions of interest (ROIs) on the map. An ideal choice of b value would be such that-

B value X ADC ~ 1.

Tissues with restricted diffusion are hyperintense in diffusion weighted images and hypointense on the corresponding ADC map. Accepted ADC values depend on the tissue being imaged and the pathology.

MRI techniques used for pulmonary diffusion weighted imaging

Takahara et al(42) used a technique a technique to perform whole body MRI using STIR sequences with higher b factors. It was also found that free breathing technique with STIR and

10 excitations produce good fat suppression and higher signal to noise ratio (SNR) than other techniques like breath hold techniques with 2 excitations and chemical shift selective pulse.

Application of DWI in lung malignancy

Malignant tumours have increased cellularity and are biologically aggressive. DWI has been used to help diagnose tumours in various organs in the body as a tool for both qualitative and quantitative assessment.

Qualitatively, the images can be visually assessed for relative increase in signal intensity of the lesion on comparison with normal tissue enabling both detection and, to some extent, characterization of the lesion (43). There have been a studies that have proven the effectiveness of DWI in helping visually, differentiate malignancy from post-obstructive lung collapse (44) and benign nodules (45) based on signal intensity. However, lesion characteristics were not typical of either and could not be used to differentiate between the two.

Quantitative assessment of the lesion can be done by ADC calculation, which is related to the diffusion of water molecules within the intracellular and extracellular components of the lesion. In most malignant lesions, the ADC values are reduced. This can be attributed to increased cellular density within the tissue. Additionally, the altered cell membranes, organelles, intracellular cytoskeleton and macromolecular composition also play a role in contributing towards diffusion restriction within these lesions. (46). Many studies have shown a significant relationship between low ADC values with renal, hepatic, prostate and certain brain tumours (47,48).

There are a few studies that have proven that the mean value of ADC for benign lesions is higher than that for malignant lesions(1,45,49). Few have also studied the relationship between

lesion to spinal cord ratio and compared with absolute ADC measurement of the lesions concluding that the latter showed better correlation (50).

A study conducted by Liu et al (50) recruited sixty two patients who underwent DWI for evaluation of benign and malignant pulmonary lesions and compared the signal intensity of the lesion with that of skeletal muscle (b=500 s/mm^2) and found no statistically significant difference between benign and malignant lesions. However, Uto et al (2009) in their study of 67 patients compared lesion to spinal cord ratio (LSR) on DWI (b=1000 s/mm^2) and ADC and found that LSR > 1.135 was found to have an accuracy of nearly 85.7 % in diagnosing malignant lesions (51). Gumustas et al (2012) later conducted a study on 62 patients who underwent DWI and the absolute signal intensity of the lesion of interest (SI) was estimated on DWI (b=1000) and signal intensity of >277 in malignant lesions showed a sensitivity of 93 %, specificity of 69 % and positive predictive value of 85 % (52).

Mori et al (2008), in a study including 140 pulmonary nodules, showed that lesions with an ADC less than 1.1×10^{-3} mm^2/s were significantly more likely to be of malignant etiology (53). Similarly Liu et al (2010) in a study including 66 patients with pulmonary nodules (12 benign and 54 malignant) showed that a cut-off ADC value of more than 1.4×10^{-3} mm^2/s to represent a benign lesion, showed a sensitivity of 83.3% and a specificity of 74.1% (50).

In the context of lung malignancies, the role of diffusion weighted magnetic resonance imaging in predicting the invasiveness of the NSCLC has also been assessed by Kanauchi et al (2009). In this study performed on a total of 41 patients with NSCLC (10 invasive and 31 non-invasive), the lesion to spinal cord ratio was found to be an independent predictor of invasive lung carcinoma with a sensitivity of 90% and a specificity of 81%. (54).

In another study which looked at the correlation of PET with diffusion weighted imaging by Tyng et al (2018), there was found to be a significant inverse correlation between ADC values on diffusion weighted MR images and SUV$_{max}$ on PET images (p<0.001).

Presence of necrosis within both malignant and infectious lesions significantly alters the ADC value. Karaman et al(55) compared the wall/ necrosis ratio of benign infectious to malignant lesions and found the cut-off value of 1.12 showing sensitivity of 100% & specificity of 98% specificity for malignancy with good intra and inter-observer reliability.

Role of DWI and ADC in differentiating types of malignancy

In order to determine disease prognosis, staging and guide treatment, lung cancer can be classified as SCLS (small cell lung carcinoma) and NSCLC (non-small cell lung carcinoma). SCLS, apart from merely, its unique histopathological appearance and immune-histochemical markers, unlike NSCLC is more aggressive, often presents with metastases or para-neoplastic syndromes at the time of diagnosis and is associated with a poorer prognosis (56). There are also significant differences between the treatment options for both types. While surgery is the preferred treatment for stages 1- 3A for NSCLC, unresectable non-small cell carcinoma required chemo-radiation (57).

Therefore, it is of vital importance to obtain a histopathological diagnosis prior to initiating treatment. This, however, poses some challenges and limitations. Trans-bronchial biopsies for peripherally located lesions and those with a diameter < 2cm, sufficient representative samples may not be obtained and sensitivity (in case of negative bronchoscopy) could be as low as ~ 40% (58) and CT guided biopsy, although more suited for peripherally located tumours is fraught with complications like pneumothorax and haemorrhage.

Also, of particular interest, is the discovery of targeted therapy for the treatment of adenocarcinoma, a type of NSCLC. Epidermal growth factor receptor (EGFR) exists on the

cell surface and is activated by binding of its specific ligands, including epidermal growth factor and transforming growth factor α (TGFα). Mutations that lead to EGFR overexpression (up regulation) or over activity have been associated with a number of cancers. Without kinase activity, EGFR is unable to activate itself, which is a prerequisite for binding of downstream adaptor proteins. Ostensibly by halting the signalling cascade in cells that rely on this pathway for growth (EGFR tyrosine kinase inhibitors), tumour proliferation and migration is diminished. (59) .

Diffusion weighted imaging, carries the inherent advantage of being non-invasive and not exposing the patient to ionizing radiation, hence its importance increased further in patients who are unable to undergo biopsy. A study conducted by Matoba et al (2007) which recruited 30 patients with lung carcinoma showed a significant difference in ADC value in squamous cell carcinoma and large cell carcinoma compared to benign lesion ($p < 0.05$), and a significantly higher ADC value in well differentiated compared to moderately and poorly differentiated carcinoma ($p < 0.05$) (60).

The purpose of this study is to characterize indeterminate pulmonary lesions on DWI images and evaluate the usefulness of ADC quantification in contributing to its diagnosis on comparison with clinical follow up, biopsy and histopathological examination or other corroborative investigations.

MATERIALS AND METHODS

Design of data collection:

- Outpatients and inpatients who undergo CECT thorax were identified.

- Those patients who satisfied the inclusion criteria for the study were identified and recruited after ruling out exclusion criteria and obtaining informed consent.

- MRI of the thorax was performed in the Radiology department with a Siemens 1.5 T MRI machine.

- The scan was reported by the principal investigator using a standardized format

- Final diagnosis was obtained through biopsy, other corroborative investigations and follow up.

- Patients without a definite final diagnosis or lost to follow up were excluded from the study.

Cases:

Patients with indeterminate pulmonary lesions based on CECT thorax in the time period between October 2016 and September 2018 (2 year period).

Methodology:

Forty seven consecutive patients with indeterminate pulmonary lesions detected on CECT thorax who fulfilled the selection criteria for the study underwent T2 weighted imaging, diffusion weighted imaging (b=0, b=500, b=1000 s/mm^2) and ADC quantification after informed consent.

Inclusion criteria:

- Patients ≥18 years of age who had undergone CECT of the thorax showing indeterminate pulmonary lesions

- Lesion with greatest diameter ≥ 1cm (nodules or mass or masses or cavity or consolidation)

- Reported as 'could be infection or malignancy'

Exclusion criteria:

- Patients who have already undergone biopsy of the lesion of interest that may alter the signal intensity of lesion on MRI.

- Patients who have already undergone any treatment in the form of surgery or chemotherapy or radiotherapy or other medical treatment that may alter the pulmonary lesion.

- Patients for whom MR imaging is contra-indicated due to the presence of aneurysmal clips, pacemakers, defibrillators that are not MRI compatible

- Patients with severe claustrophobia, conditions that preclude ability to lie supine within the gantry (examples: severe orthopnoea secondary to pulmonary, cardiac or other causes), uncooperative patients or those requiring sedation or anaesthesia to undergo the procedure

- Patients who have both infection and malignant lung pathology

- Patients with motion artefacts that would impair image interpretation

Outcome measures:

DWI images: A region of interest (ROI) was chosen from the pulmonary lesion (largest possible diameter with no area of necrosis or foci of air) and another from the spinal cord (at least 10mm2) and the LSR was estimated. The signal intensity of the pulmonary lesion (in an

area devoid of necrosis or foci of air) was also visually compared to that of the thoracic skeletal muscle and noted as

- 1- hypointense
- 2- isointense
- 3- hyperintense

ADC map: Rounded or elliptical ROI with an area of at least 10mm² was chosen from the solid area of the lesion with no areas of necrosis or foci of air and another ROI from an area of necrosis if present in the lesion.

Study population recruitment:

Sample size calculation:

Based on study of Gumustas Sevtap et al (20), the formula for comparison of means between the two groups

$$N = \frac{(Z_{1-a/2} + Z_{1-\beta/2})^2 \, 2 \, \sigma^2}{(M1 - M2)^2}$$

$Z_{1-a/2} = Z$ value for the required alpha error

$Z_{1-\beta/2} = Z$ value for the required beta error

σ = known standard deviation of the measure

(M1-M2) = desired precision = difference in the known mean values of the two groups

N = Number of observations in each group (benign versus malignant) = 16 per group

Sample selection:

The study was conducted in the Department of Radiology, Christian Medical College and Hospital, Vellore from the period between October 2016 and September 2018.

Forty seven consecutive patients were included in this MRI study of indeterminate pulmonary lesions who fulfilled the inclusion criteria without exclusion criteria. The patients took part voluntarily and signed the informed consent.

Sampling strategy:

Consecutive patients fulfilling the eligibility criteria and willing to take part in the research project voluntarily were recruited for the study

104 patients who fulfilled inclusion criteria

- Patients >=18 years of age
- Patients with pulmonary lesions that are indeterminate on CECT
- Greatest diameter of the pulmonary lesion >= 1cm

52 patients exluded

- Patients who had already undergone biopsy of the lesion of interest
- Patients who had already started chemotherapy/ medical therapy
- Patient unable to lie supine within the gantry due to orthopnoea
- Patients unwilling for biopsy and lost to follow up

52 patients underwent MRI

5 patient with MR images suboptimal for interpretation

47 patients with MR images optimal for interpretation

20 malignant lesions

27 benign lesions

Design of data collection:

Prospective observational study

Data sources:

The CECT thorax images and report of the patients who underwent scan in the department of Radiology were assessed by the principal investigator and guide for the presence of indeterminate pulmonary lesions to identify cases to be included in the study.

The final diagnosis was obtained by histopathological examination of the biopsy specimen from the lesion obtained by image guidance or bronchoscopy or surgery and other corroborative investigations like sputum smear or culture, blood culture, serum markers and by follow up imaging documentation of resolution of the lesion on treatment with antibiotics or steroid.

Thoracic MRI study:

Machine: 1.5T Siemens MRI machine

MRI sequences: With the patient in supine position, the following sequences were obtained:

1. Respiratory gated T2-weighted images were obtained in the axial plane using the following parameters: TE/ TR-92/2000ms; matrix-324 x 384; slice thickness -6 mm; gap-0.6 mm.

2. Diffusion weighted images (DWI) was obtained with b values of 0, 500 and 1000 s/mm^2

3. ADC quantification was done using an in-built software

In the diffusion weighted images, the signal intensity of the lesion of interest (without necrotic areas or foci of air) was compared to that of the thoracic skeletal muscle as being hypointense, isointense or hyperintense.

Diffusion weighted images (b=0, b=500 and b=1000 s/mm^2) were then taken and the lesion to spinal cord signal intensity ratio was then estimated.

ADC value was quantified from the regions of interest within the solid and necrotic components of the lesion. The results were then compared to the final diagnosis obtained by biopsy, other corroborative investigations and clinical findings.

Personnel:

Reporting of T2 weighted, diffusion weighted images and ADC maps was done by the principal investigator and approved by the thesis guide (Professor).

The biopsy of the lesion was performed under bronchoscopic guidance (Pulmonary medicine department) or ultrasound or CT guidance (Radiology department)

The histopathological and cytological examination of the specimens were done be done by a pathologist (Pathology department)

The culture of the specimen was done in the microbiology department.

Statistical methods:

All baseline continuous variables were expressed in terms of mean ± standard deviation and all categorical variables were reported using frequencies and percentages. The mean LSR and ADC between benign and malignant lesions and their subgroups were compared using the independent samples T- test. Differences were considered significant at $p < 0.05$. ROC curves were then plotted and cut-off values obtained to differentiate benign and malignant

pulmonary lesions and their respective sensitivities and specificities were calculated. All the statistical analysis were performed using SPSS 16.0

Interpretation

During interpretation of the MR images, the principal investigator and thesis guide were blinded to the results of biopsy, corroborative investigations and details of clinical follow up.

The study comprised of a total of 47 patients with indeterminate pulmonary lesions detected on CECT of the thorax.

Demographic profile of the participants

The patients enrolled in this study were of the age group 24-79 years with mean age of 50 years. The largest group of patients were in the age group 50-59 years (Figure 7).
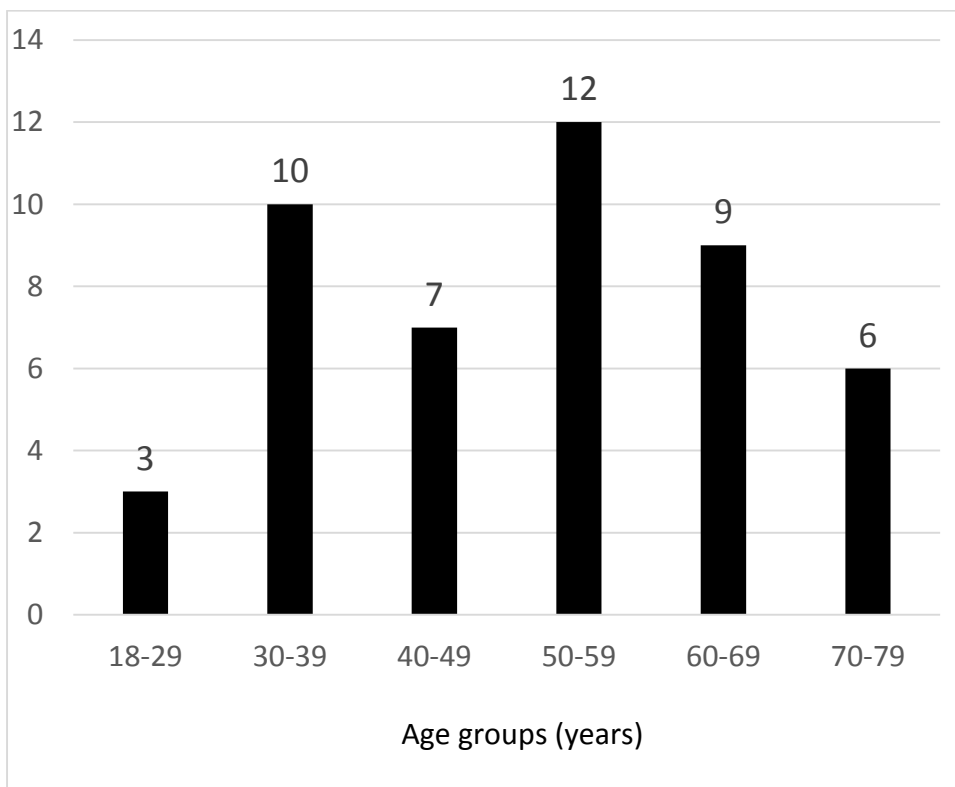
Figure 7: Column graph demonstrating age distribution of patients

Of the total of 47 patients enrolled, there were 32 men and 15 women. The patients for the study were referred from the departments of general medicine, pulmonary medicine and

medical oncology. The distribution of patients based on the department of referral is as given in Table 1.

Table 1: Distribution of patients enrolled in the study according to department of referral

Department of Referral	No. of Patients	Percentage (%)
General Medicine	8	17.02
Pulmonary Medicine	34	72.34
Medical Oncology	5	10.64
Total	47	100.00

Final diagnosis

Of the total of 47 patients, 43 underwent biopsy. The final diagnosis was obtained for 2 patients by confirmation on sputum culture and TB PCR test and for the remaining 2 patients on follow up imaging within a month showing significant resolution of the lesion on treatment with short course of empirical non-antimycobacterial antibiotics.

Among the 43 patients who underwent biopsy, 32 underwent CT guided biopsy, 10 underwent transbronchial biopsy and 1 underwent thoracoscopic guided biopsy (Figure 8).
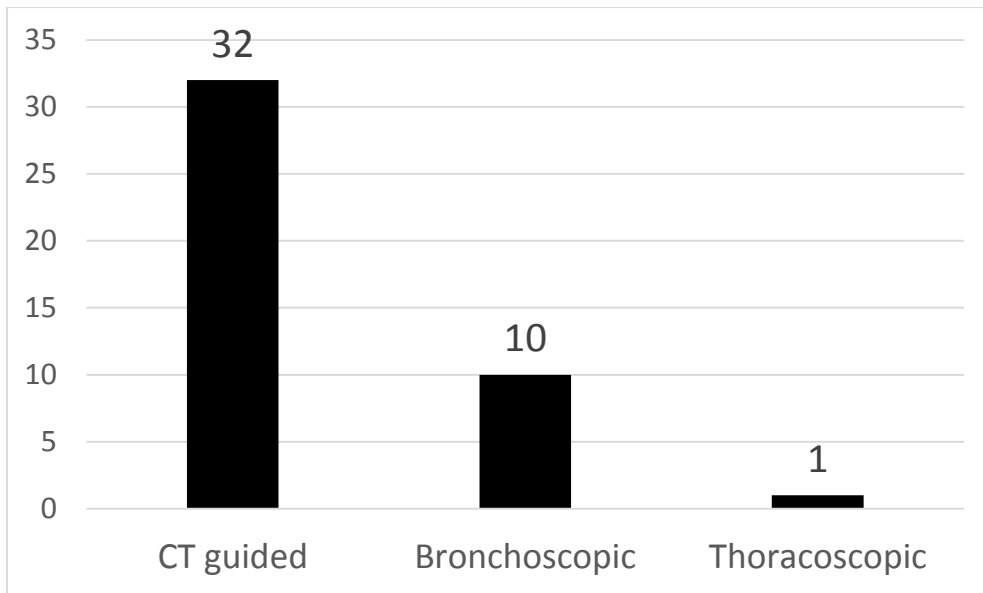
Figure 8: Distribution of patients according to method of biopsy (N=43)

Of the 47 patients, the lesions in 27 patients (57.4%) were confirmed as benign and the lesions in 20 patients (42.6%) were confirmed as malignant.
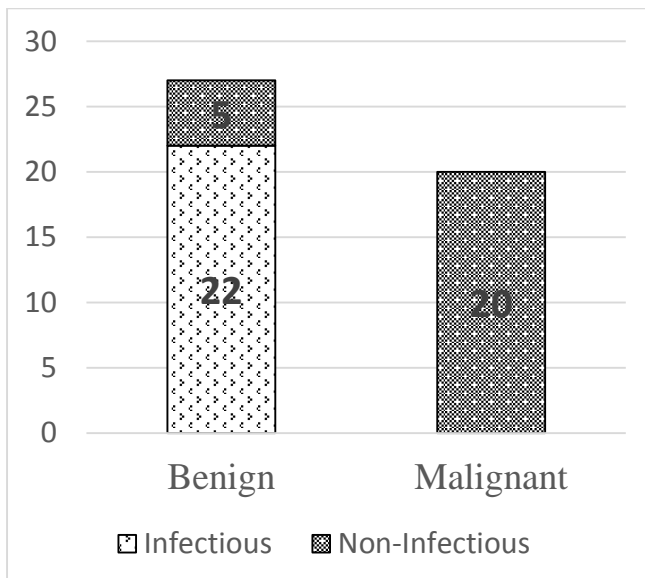
Figure 9: Stacked column graph depicting division of patients based on diagnostic categories

Among the 20 patients with malignant lesions, the types of malignant lesions included were as noted in Table 2.

Table 2: Distribution of type of malignant pulmonary lesions based on biopsy (N=20)

Type of malignancy	No. of patients	Percentage (%)
Adenocarcinoma	11	55
Squamous cell carcinoma	4	20
Undifferentiated carcinoma	2	10
Lymphoma	2	10
Large cell carcinoma	1	5
Total	20	100

Among the 11 patients with biopsy proven adenocarcinoma of the lung, testing for EGFR mutations was performed on 6 patients, 1 of which tested positive and 5 were negative.

Among the 20 patients with pulmonary lesions secondary to an infective cause, the distribution of causative pathogens was as noted Figure 11. Fifty percentage of these cases were tuberculosis.
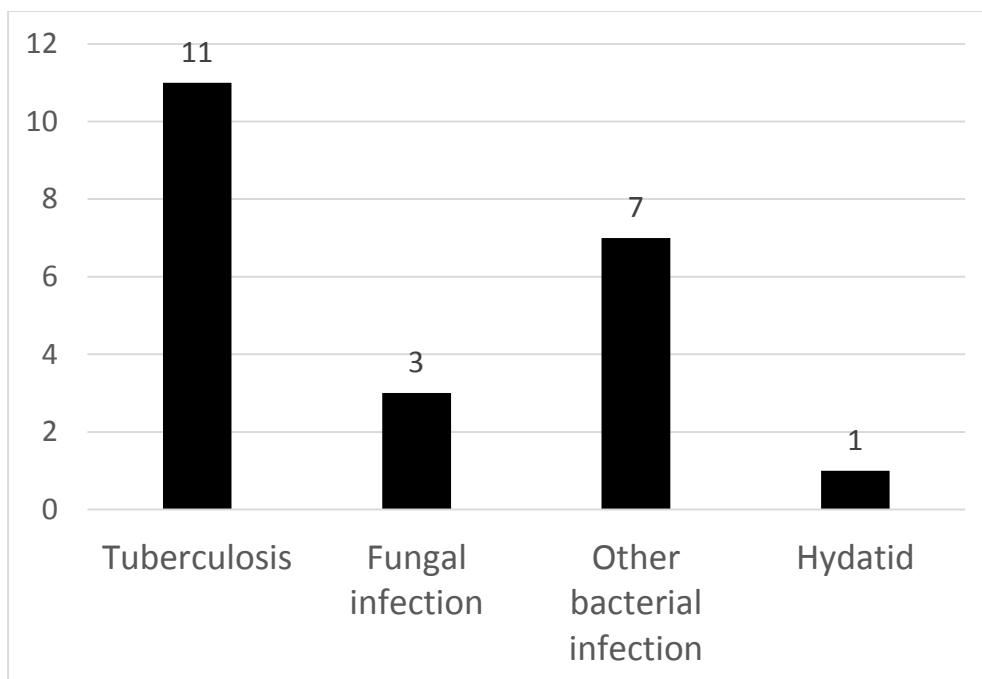
Figure 10: Distribution of infection based on the causative pathogen

Among the cases of non-infectious benign pulmonary lesions, there was 1 case of pulmonary amyloidosis and 1 case of IgG4 disease, the rest being non-specific inflammatory lesions.

Clinical Profile

The mean duration of symptoms was 9.31 and 7.70 months for benign and malignant lesion with no significant difference between the two groups (p = 0.637). 29.6% of the patients with benign pulmonary lesions and 40% of the patients with malignant pulmonary lesions had history of smoking. Three of the 11 cases of adenocarcinoma (27.2%) had history of smoking as compared to 3 of the 4 cases of squamous cell carcinoma (75%). The symptom profile of the patients included in the study and the distribution of smokers in each of these groups are as described in tables 3 and 4 respectively.

Table 3: Symptom profile of patient with benign and malignant pulmonary lesions

Symptom profile	Benign	Malignant
Cough	25(92.6%)	17(85%)
Expectoration	17(63%)	7(35%)
Chest pain	8(29.6%)	6(30%)
Breathlessness	16(59.3%)	10(50%)
Haemoptysis	16(59.3%)	7(35%)
Fever	9(33.3%)	5(25%)
Sig. weight loss	12(44.4%)	8(40%)
Total	27	20

Table 4: Distribution of smokers versus non-smokers

	Benign	Malignant
Non-smoker	19	12
Smoker	8	8
Total	27	20

Characteristics of the pulmonary lesions on CT

Of the 47 patients, the pulmonary lesion (in case of multiple, the largest lesion) were seen to be located predominantly in the right lung (59.5%)) and lower lobes (46.8%). Most lesions were solitary (73%)) and unilateral 91.5%). The average of the maximum diameters of the lesions was 5.28cm. 44.4% of benign and 25% of malignant lesions had areas of necrosis.

Of the total of 47 cases, 40 (85.1%) had ipsilateral mediastinal lymphadenopathy, 34 (72.3%) cases had ipsilateral hilar lymphadenopathy, 10 (21.3%) had contralateral mediastinal lymphadenopathy and 2 (4.2 %) had contralateral hilar lymphadenopathy. 11 patients (23.4 %) had associated with pleural effusion.
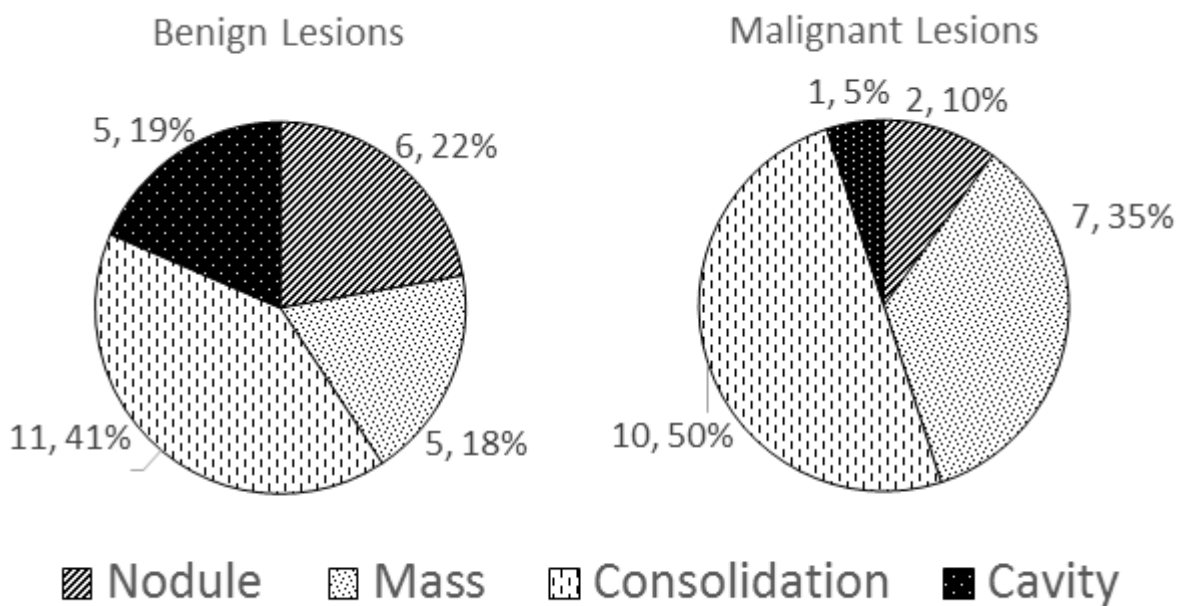
Figure 11: Pie charts demonstrating the distribution of type of lesion in benign versus malignant lesions

Of the 27 benign pulmonary lesions, most lesions were areas of consolidation (40.74%) and nodules (22.2%)). A few cases of infection and one case of IgG4 disease presented as mass like

lesions. The distribution of benign pulmonary lesions according to CT appearance is as shown in Table 5.

Table 5: CT appearance of benign lesions

Final Diagnosis	Type of lesion				Total
	Nodule	Mass	Consolidation	Thick walled cavity	
Tuberculosis	3	1	5	2	11
Fungal infection	0	1	1	1	3
Other bacterial infection	2	1	3	1	7
Non-specific inflammation	1	0	1	1	3
Hydatid	0	1	0	0	1
Amyloidosis	0	0	1	0	1
IgG4 disease	0	1	0	0	1
Total	6	5	11	5	27

Of the 20 malignant lesions, most cases of adenocarcinoma presented as areas of consolidation (54.5%). The distribution of various malignant pulmonary lesions according to their CT appearance is as shown in Table 6.

Table 6: CT appearance of malignant lesions

Final Diagnosis	Type of lesion				Total
	Nodule	Mass	Consolidation	Thick walled cavity	
Adenocarcinoma	2	3	6	0	11
Squamous cell carcinoma	0	2	1	1	4
Large cell carcinoma	0	1	0	0	1
Lymphoma	0	1	1	0	2
Undifferentiated carcinoma	0	0	2	0	2
Total	2	7	10	1	20

Characteristics of the pulmonary lesions on MRI

Most benign and malignant lesions appeared as hyperintense on DWI with no statistically significant difference on b=500 s/mm^2 images (p value = 0.590) and b= 1000 s/mm^2 images (p value = 0.590) (Tables 7, 8).

Table 7: Comparison of signal intensity of lesion to that of thoracic skeletal muscle in benign versus malignant pulmonary lesions on DWI with b=500 s/mm^2

	Signal Compared To Skeletal Muscle (b=500 s/mm^2)			Total	p value
	Hypointense	Isointense	Hyperintense		
Benign	1	7	19	27	
Malignant	0	4	16	20	0.590
Total	1	11	35	47	

Table 8: Comparison of signal intensity of lesion to that of thoracic skeletal muscle in benign versus malignant pulmonary lesions on DWI with b=1000 s/mm^2

	Signal Compared to Skeletal Muscle (b=1000 s/mm^2)			Total	p value
	Hypointense	Isointense	Hyperintense		
Benign	1	7	19	27	
Malignant	0	4	16	20	0.590
Total	1	11	35	47	

On comparing benign (N=27) versus malignant (N=20) lung lesions, there was a statistically significant difference between the signal intensity values of the solid component on b=1000 s/mm^2 (p value =0.002; 95% CI 105.22 to 2.04 s/mm^2), LSR on b=500 s/mm^2 (p value=0.002;

95% CI 0.97 to 0.24) and b= 1000 s/mm^2 (p value= 0.001; 95% CI 1.06 to 0.29) and ADC value of the solid component (p value= 0.006; 95% CI 0.969 to 0.079 x 10^{-3} mm^2 /s) as demonstrated in Table 9.

There was no statistically significant difference between signal intensity values of malignant and non-malignant lesions on b=500 s/mm^{2}images (p value= 0.059; CI =105.22 to 2.04).

Table 9: Comparison of signal intensity of solid component of lesion, LSR and ADC of solid component between malignant & benign lesions using the independent sample T test (N=47)

		N	Mean	SD	p value	95% CI	
						Upper	Lower
SI value on DWI (b=500 s/mm^2)	Benign	27	132.17	86.49	0.059	105.22	2.04
	Malignant	20	183.76	95.14			
SI value on DWI (b=1000 s/mm^2)	Benign	27	72.01	38.11	0.002	80.69	18.13
	Malignant	20	121.42	67.65			
LSR(DWI b=500 s/mm^2)	Benign	27	0.92	0.45	0.002	0.97	0.24
	Malignant	20	1.52	0.78			
LSR(DWI b=1000 s/mm^2)	Benign	27	0.90	0.43	0.001	1.06	0.29
	Malignant	20	1.58	0.86			
ADC (sol.) (X 10^{-3} mm^2/s)	Benign	27	1.438	0.465			
	Malignant	20	1.072	0.399	0.006	0.111	0.621
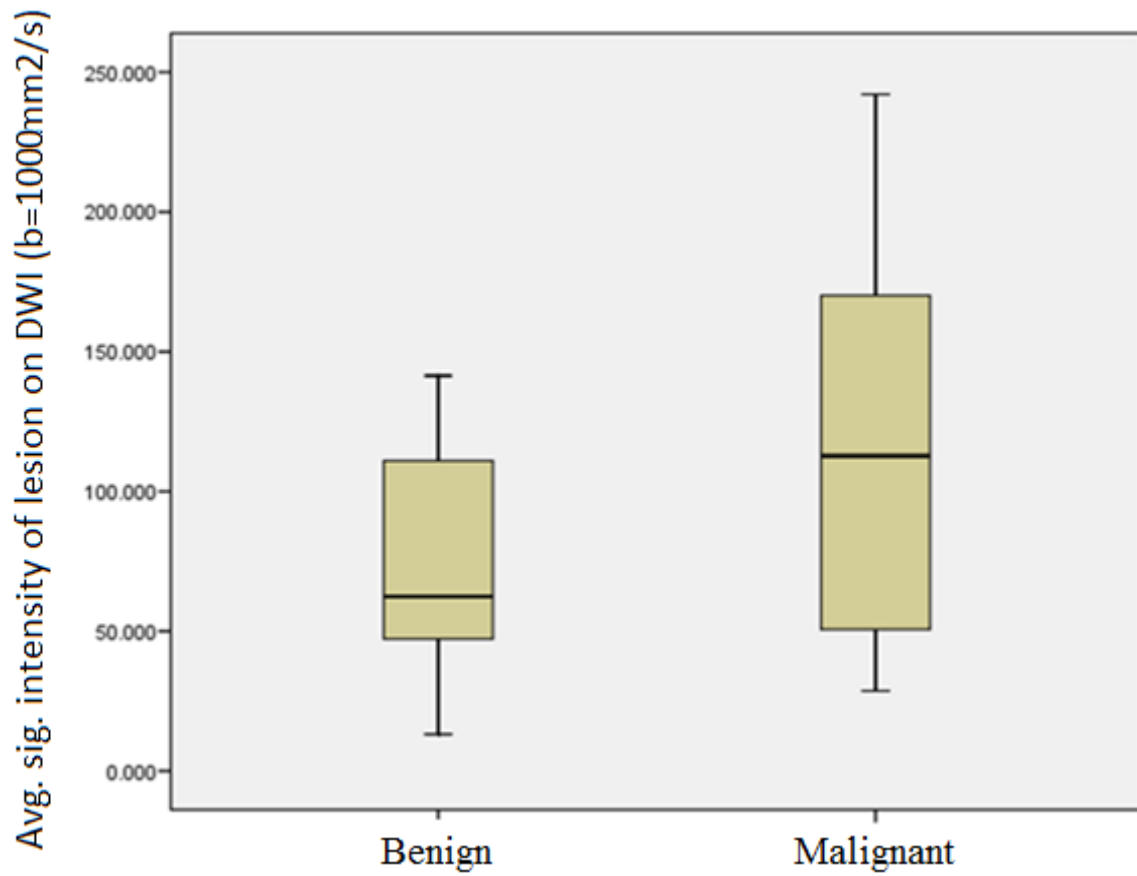
Figure 12: Box plot showing significant difference in average signal intensity of the solid component in benign versus malignant lesions on DWI (b= 1000 s/mm^2) (p value =0.002; 95% CI 18.13 to 80.69)
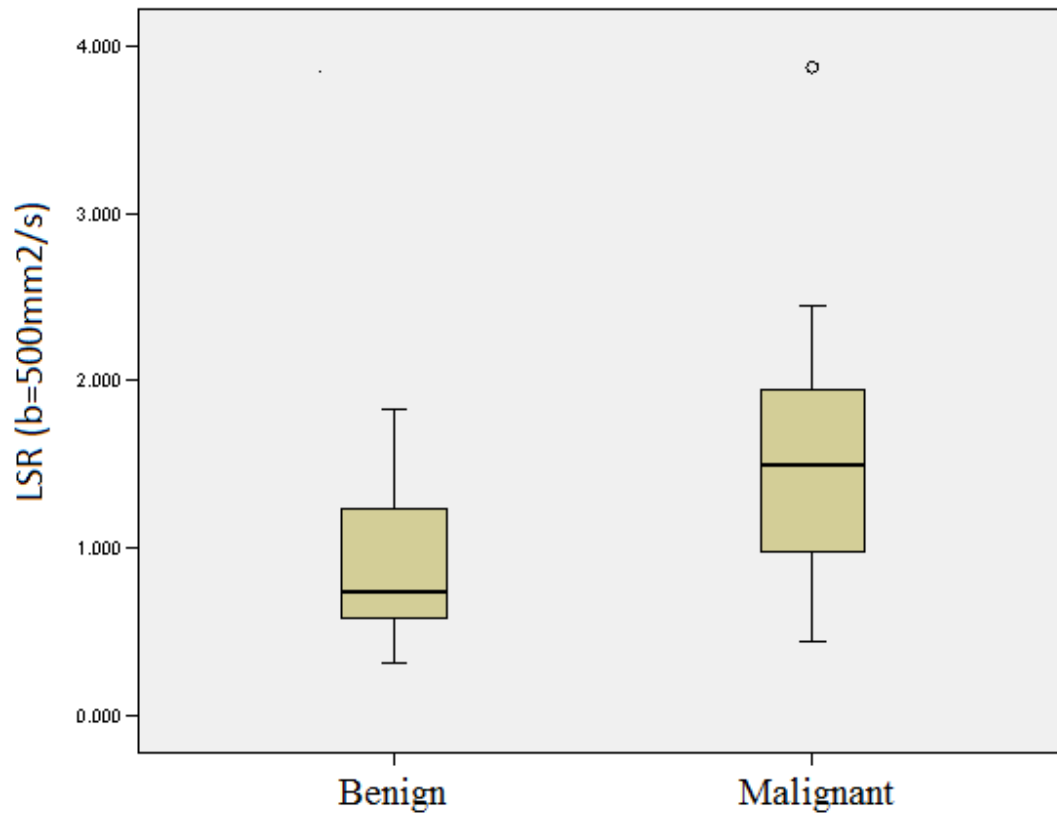
Figure 13: Box plot showing significant difference in LSR on DWI (b= 500 s/mm^2) in benign versus malignant lesions (p value=0.002; 95% CI 0.97 to 0.24)
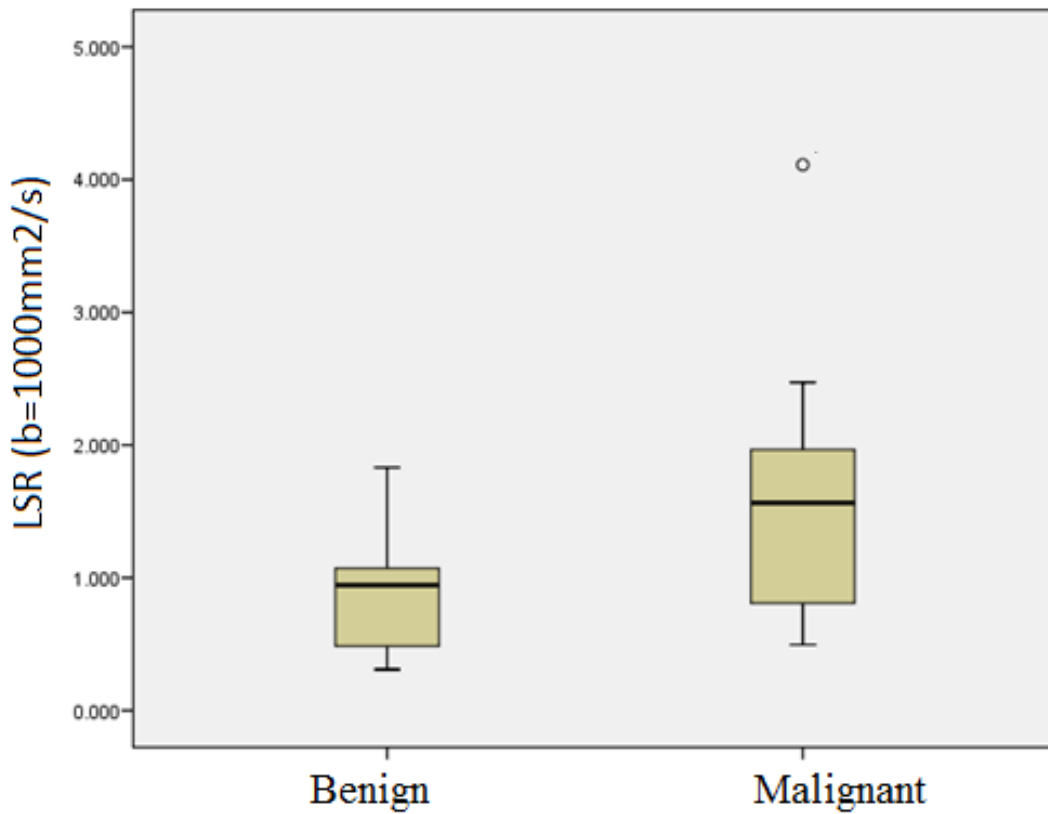
Figure 14: Box plot showing significant difference in LSR on DWI (b= 1000 s/mm^2) in benign versus malignant lesions (p value= 0.001; 95% CI 0.29 to 1.06)

The outlier values of 3.875 on LSR (b=500 s/mm^2) and 4.111 on LSR (b=1000 s/mm^2) were that of a cases of mucinous type of adenocarcinoma.
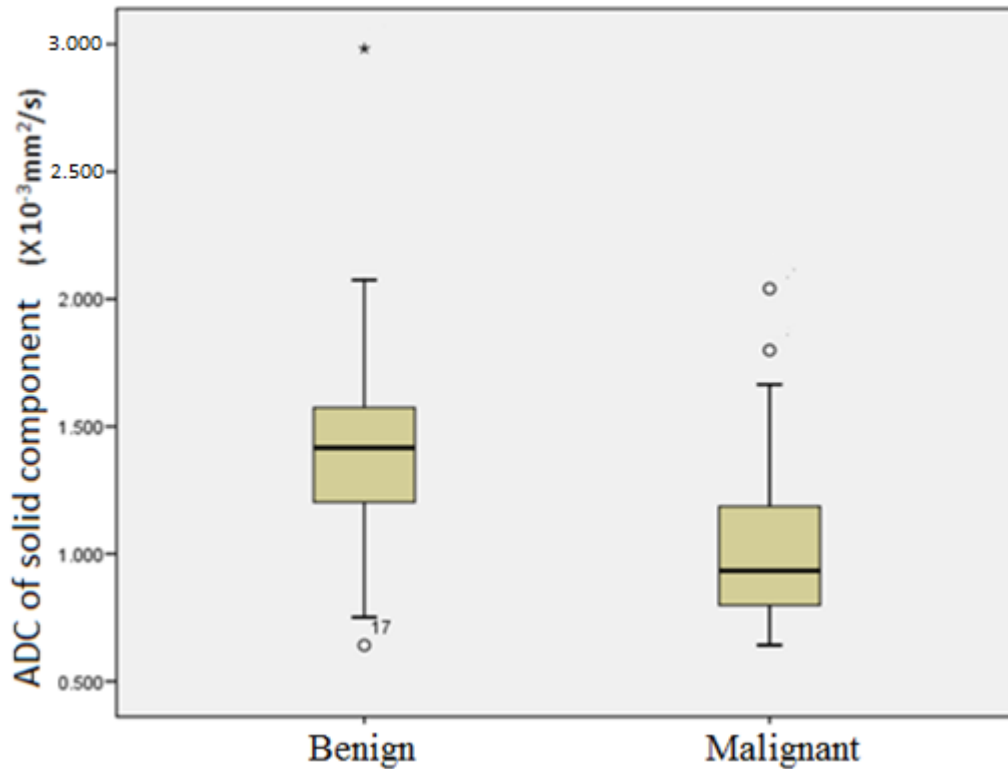
Figure 15: Box plot showing significant difference in the ADC of the solid component in benign versus malignant lesions (p value= 0.001; 95% CI 0.111 to 1.621 x 10^{-3} mm^2/s)

Of the 20 cases of malignancy, some malignant lesions like mucinous adenocarcinoma (2/4) and squamous cell carcinoma (2/5) showed ADC values higher than the said cut-off value and among the 27 cases of benign lesions, few cases of tuberculosis (2/11), fungal infection (1/3) and a case of amyloidosis showed ADC values lower than that of the cut-off.

Of the total of 47 cases, 12 of the 27 benign lung lesions and 5 of the 20 malignant lung lesions had areas of necrosis. There was found to be no significant difference in the apparent diffusion coefficient of the necrotic components in the two groups (p value= 0.132; 95% CI 1.393 to 0.201 x 10^{-3} mm^2/s).

Of the 27 cases of benign pulmonary lesions, 11 lesions were due to tuberculosis and 10 were due to non-tubercular infections (fungal, hydatid, other bacterial infections) and other

conditions like amyloidosis and IgG4 disease. There was found to be no significant difference in signal intensity on DWI for b=500 s/ mm^2 and b=1000 s/ mm^2, lesion to spinal cord ration for b=500 s/ mm^2 and b=1000 s/ mm^2 images or in the ADC values of the solid component of the tuberculous versus other benign lesions, as shown in Table 10.

Table 10: Comparison of mean signal intensity on DWI (b=500 and b=1000 s/ mm^2), LSR (b=500 and b=1000) and ADC (solid component) between tuberculosis and non-tuberculous lesions using the independent samples T-test (N=24)

		N	Mean	SD	p value	95% CI	
						Upper	Lower
SI value on DWI (b=500 s/ mm^2)	Tuberculosis	11	107.87	75.679			
	Other benign lesions	16	148.88	91.756	0.233	110.13	28.11
SI value DWI (b=1000 s/ mm^2)	Tuberculosis	11	67.7	41.509			
	Other benign lesions	16	74.981	36.688	0.635	38.49	23.93
LSR (DWI b=500 s/ mm^2)	Tuberculosis	11	0.937	0.449			
	Other benign lesions	16	0.903	0.465	0.853	0.337	0.40
LSR (DWI b=1000 s/ mm^2)	Tuberculosis	11	1.041	0.396			
	Other benign lesions	16	0.805	0.431	0.163	0.102	0.57
ADC (solid component) x 10^{-3} mm^2/s	Tuberculosis	11	1.326	0.430			
	Other benign lesions	16	1.515	0.486	0.307	0.56	0.18

Among the 20 malignant lung lesions, there was also found to be no significant differences in the above parameters between adenocarcinoma and other malignancies as demonstrated in Table 11.

Table 11: Comparison of means of signal intensity on DWI (b=500 and b=1000), Lesion to spinal cord ratio (b=500 and b=1000 s/ mm^2) and ADC (solid component) between adenocarcinoma and other malignancies using the independent samples T-test (N=13)

		N	Mean	SD	p value	95% CI	
						Upper	Lower
SI value on DWI (b=500 s/ mm^2)	Adenocarcinoma	11	169.93	98.72	0.292	147.8	47.38
	Other malignancies	7	220.14	89.07			
SI value on DWI (b=1000 s/ mm^2)	Adenocarcinoma	11	114.03	73.71	0.415	97.13	42.1
	Other malignancies	7	141.54	56.97			
LSR (DWI b=500 s/ mm^2)	Adenocarcinoma	11	1.52	0.96	0.872	0.89	0.77
	Other malignancies	7	1.58	0.49			
LSR (DWI b=1000 s/ mm^2)	Adenocarcinoma	11	1.61	1.09	0.994	0.93	0.93
	Other malignancies	7	1.61	0.47			
ADC (solid component)	Adenocarcinoma	11	1.06	0.45	0.598	0.54	0.32
	Other malignancies	7	1.17	0.35			

In differentiating benign and malignant pulmonary lesions, using diffusion weighted imaging, the highest sensitivity was achieved with an ADC cut-off of 1.248×10^{-3} mm^2/s (sensitivity - 80%; specificity~ 74.1%) (Table 18) and the highest specificity was achieved with LSR on DWI (b=1000 s/ mm^2) cut-off value of 1.275 (sensitivity ~ 70 %; specificity ~85.2 %) (Table 17). The ROC curves for LSR (b= 500 s/ mm^2 and b= 1000 s/ mm^2) and ADC are as shown in Figures 12, 13 and 14 respectively.
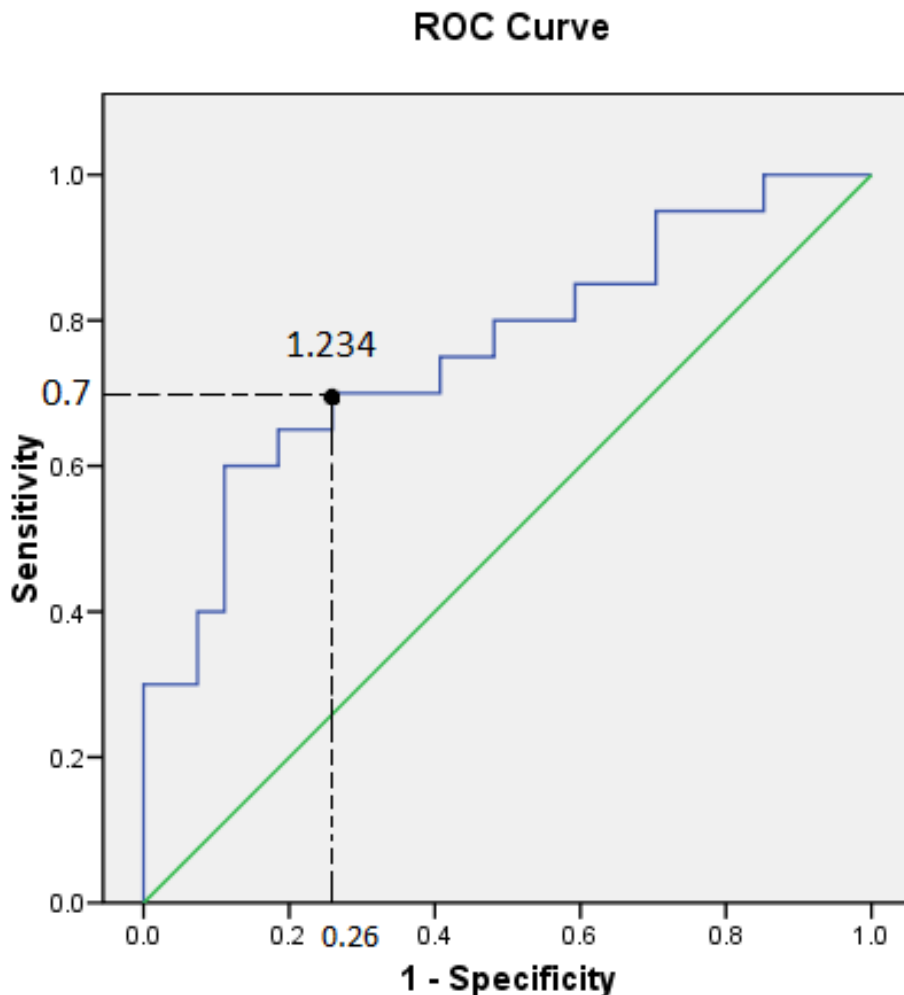
Figure 16: ROC curve for diagnostic performance of LSR (on DWI b=500 s/ mm^2) for differentiation of malignant from benign pulmonary lesions. Cut-off value of 1.234 had a 70.0% sensitivity and 74.1% specificity for differentiating the two. (AUC= 0.761)

Table 12: Diagnostic performance of LSR values on DWI (b=500 s/ mm^2) for differentiation of malignant from benign pulmonary lesions (N=47)

Area under the curve	0.761
LSR (b=500 s/ mm^2)	1.234
False positive	7
False negative	6
Sensitivity	70%
Specificity	74.1%
Accuracy	72.34%
Pos. predictive value	68.2%
Neg. predictive value	76%
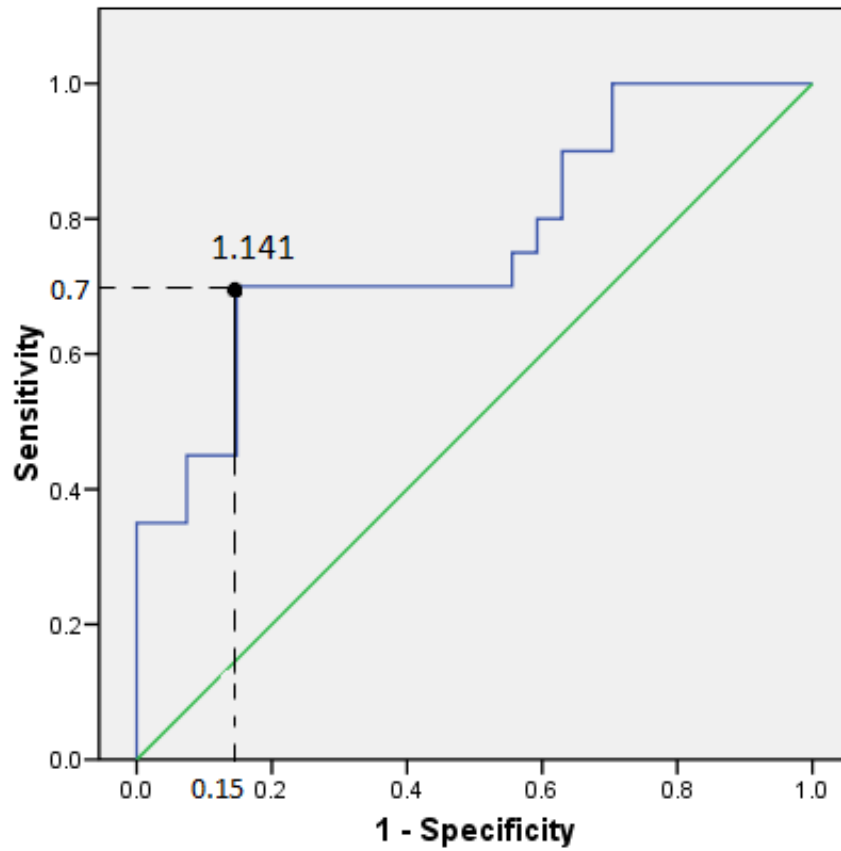
Figure 17: ROC curve for diagnostic performance of LSR (on DWI b=1000 s/ mm^2) for differentiation of malignant from benign pulmonary lesions. Cut-off value of 1.141 had a 70% sensitivity and 85.2% specificity for differentiating the two (AUC = 0.765)

Table 13: Diagnostic performance of LSR values for differentiation of malignancies from benign pulmonary nodules in DWI b=1000 s/ mm^2 images (N=47)

Area under the curve	0.765
LSR (b=1000 s/ mm^2)	1.141
False positive	4
False negative	6
Sensitivity	70%
Specificity	85.20%
Accuracy	78.72%
Pos. predictive value	77.78%
Neg. predictive value	79.31%
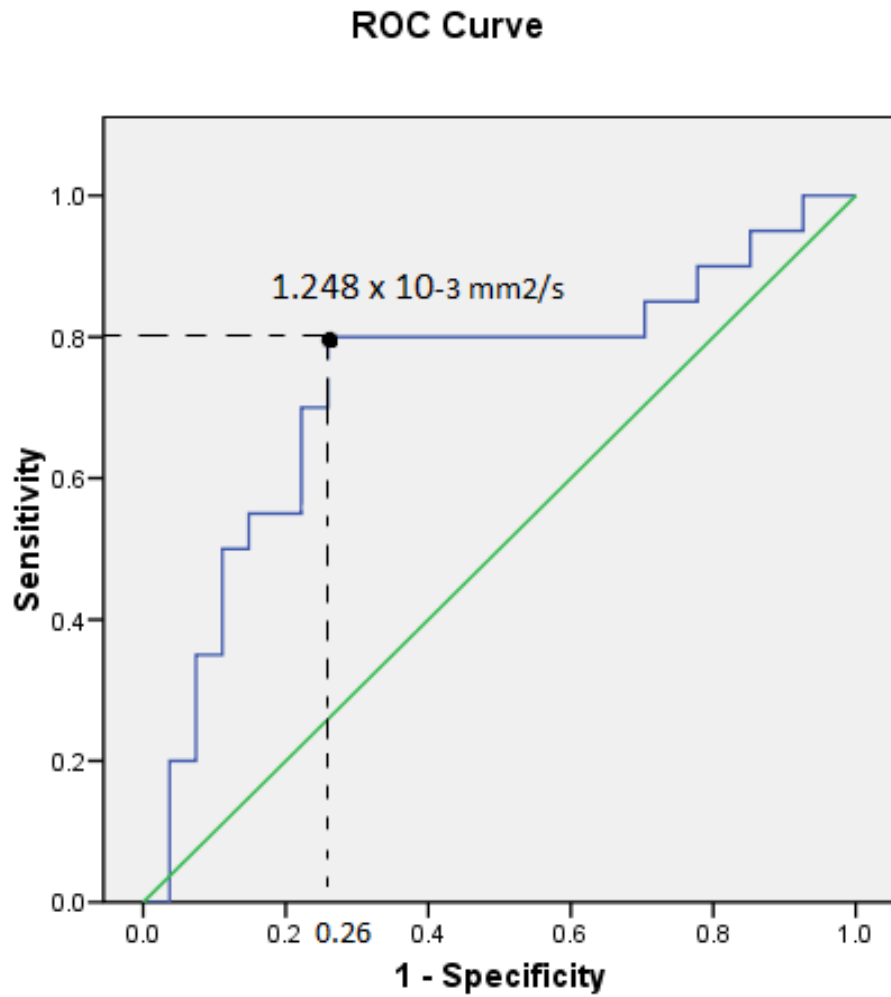
Figure 18: ROC curve for diagnostic performance of ADC values for differentiation of malignancies from benign pulmonary lesions. Cut-off value of 1.248 X 10^{-3} mm^2/s had a 80% sensitivity and 74.1% specificity for differentiating the two. (AUC= 0.735).

Table 14: Diagnostic performance of ADC values (from the solid component of the lesion) for differentiation of malignancies from benign pulmonary lesions (N=47)

Area under the curve	0.705
ADC cut off	1.248×10^{-3} mm^2/s
False positive	7
False negative	4
Sensitivity	80%
Specificity	74.1%
Accuracy	76.6%
Pos. predictive value	69.6%
Neg. predictive value	83.3%

In order to improve the overall sensitivity of detection of malignancy in an indeterminate pulmonary lesion, the cut-off values for LSR on DWI (b=1000 $\times 10^{-3}$ mm^2/s) and the ADC value were tested in parallel using 'AND' and 'OR' operators and the results are as described in Table 18. If the criterion for diagnosing malignant pulmonary lesion was both to have an LSR (b=1000 s/ mm$^{2)}$) >= 1.141 and ADC (solid component) value of <= 1.248×10^{-3} mm^2/s, the specificity of the test was raised to 96.2%. However, if the criteria for diagnosing the same was to have either of the two, the sensitivity of the test was raised to 94%.

Table 15: Testing of LSR (b=1000 s/ mm^2) and ADC cut-off values obtained in parallel

	Sensitivity (%)	Specificity (%)
Using the 'AND' operator	56.0	96.2
Using the 'OR' operator	94.0	63.1

Case 1:

61 year old man with chronic idiopathic thrombocytopenic purpura on treatment with cough

and breathlessness for 2 weeks
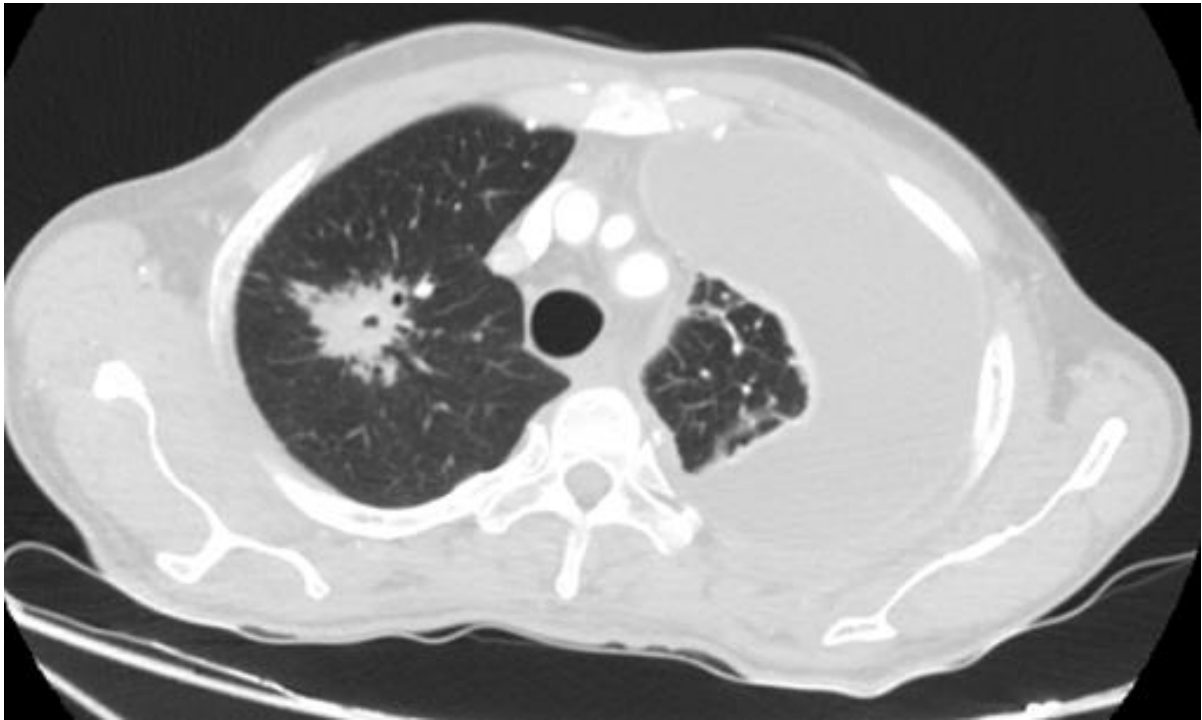
Figure 19: CECT axial section showing an irregular lesion in the right upper lobe with spiculated margins
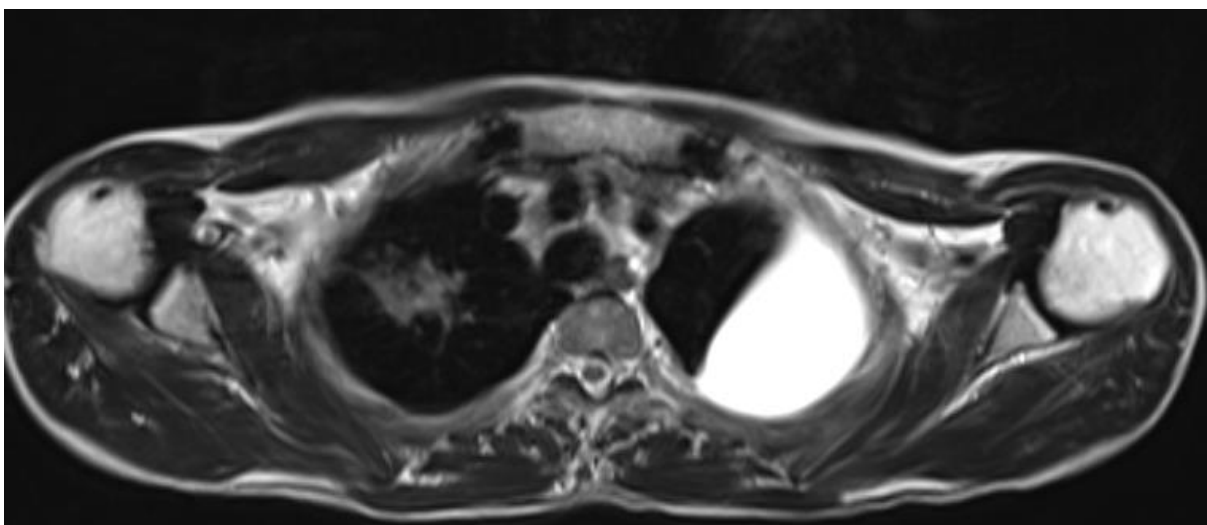
Figure 20: T2W MR axial section showing an irregular heterogeneously T2 isointense lesion in the right upper lobe
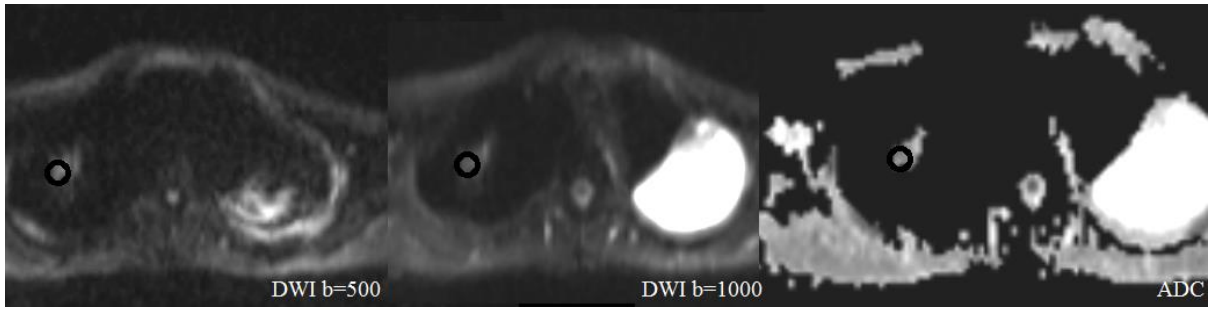
Figure 21: Diffusion weighted images showing no diffusion restriction (isointense on DWI and ADC images). The values obtained from ROI placed within the solid areas shows the following values.

Lesion to spinal cord ratio (b=500) = 0.481 (< 1.234) and lesion to spinal cord ratio (b=1000) = 0.731 (<1.141)

ADC = 1.287 x 10^{-3} mm^2/s (>1.243 X 10^{-3} mm^2/s)

Final diagnosis = Tuberculosis

Case 2:

60 year old smoker with an incidentally detected pulmonary nodule
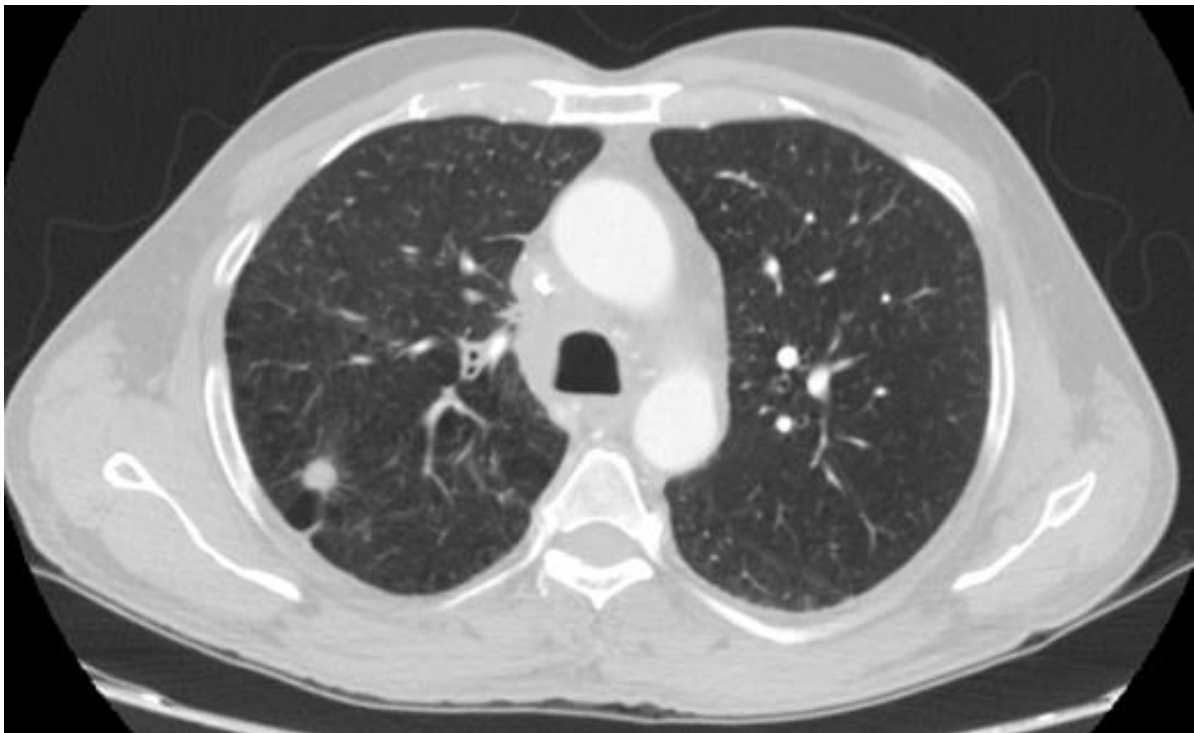
Figure 22: CECT axial section HR cuts shows a solitary pulmonary nodule in the right lower lobe
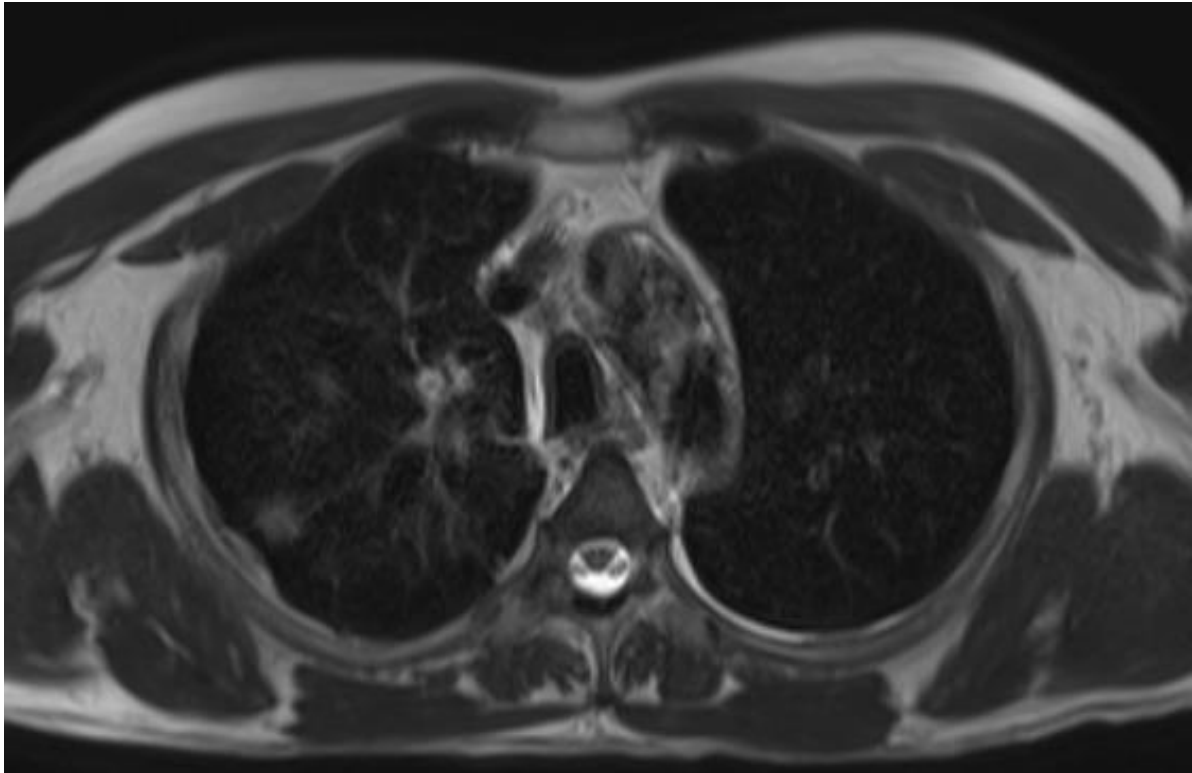
Figure 23: T2W MR axial section showing an T2 isointense nodule in the right lower lobe
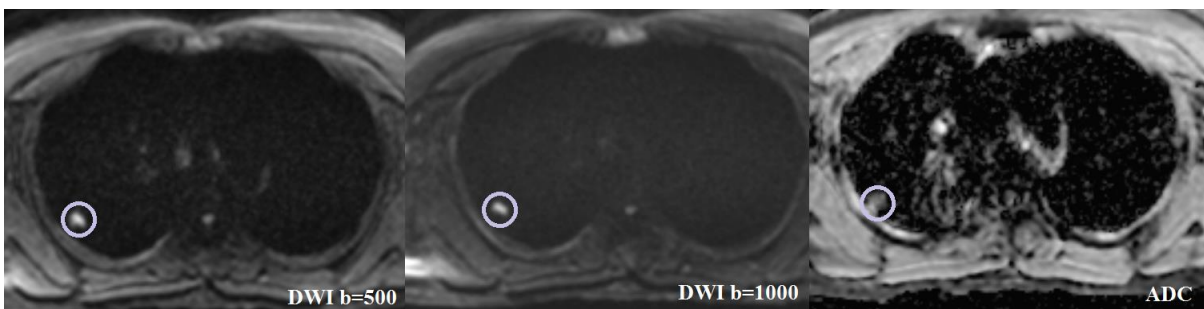
Figure 24: Diffusion weighted images showing diffusion restriction (hyperintense on DWI with corresponding dark areas on ADC).The values obtained from ROI placed within the solid area shows the following values.

Lesion to spinal cord ratio (b=500) = 2.028 (> 1.234) and lesion to spinal cord ratio (b=1000) = 2.472 (>1.141)

ADC = 1.033 X 10^{-3} mm^2/s (<1.243 X 10^{-3} mm^2/s)

Final diagnosis = Squamous cell carcinoma

Case 3:

A 36 year old man with history of cough and haemoptysis for 1 month.

Figure 25: CECT axial section showing an irregular heterogeneously enhancing lesion in the left upper lobe with central non-enhancing necrotic areas.
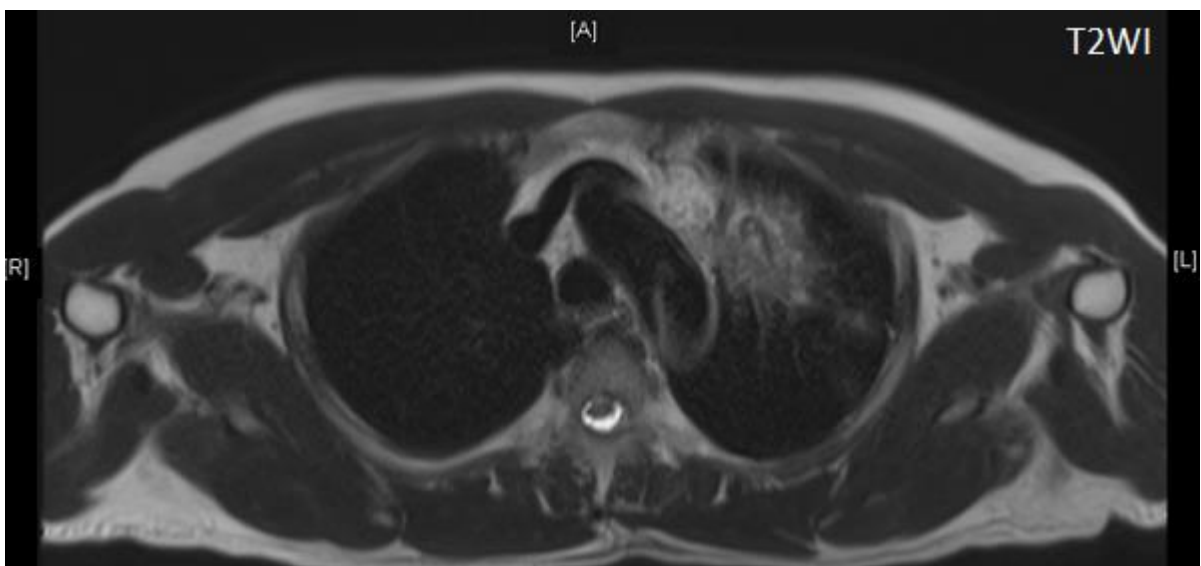
Figure 26: T2W MR axial section showing an irregular heterogeneously T2 hyperintense lesion in the left upper lobe with central T2 hypointense areas.
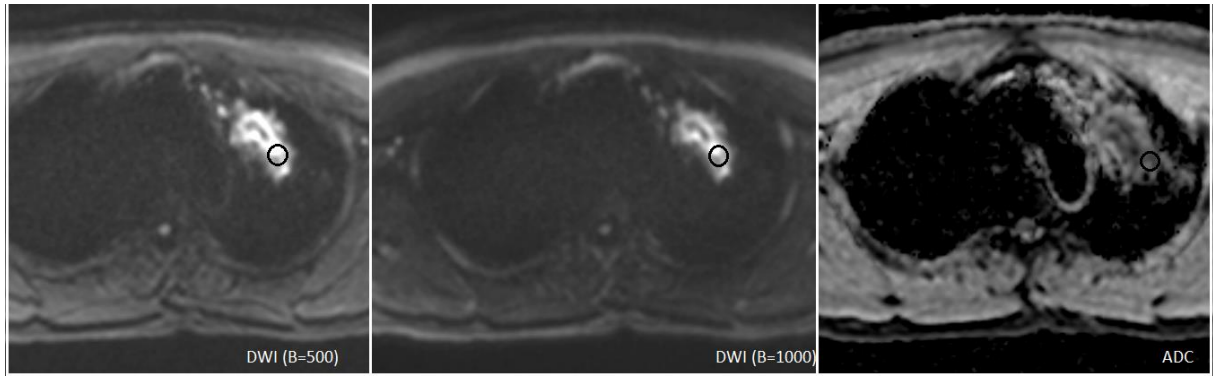
Figure 27: Diffusion weighted images showing peripheral diffusion restriction (hyperintense on DWI with corresponding dark areas on ADC) with central T2W hypointense areas showing no restriction. The values obtained from ROI placed within the solid areas shows the following values.

Lesion to spinal cord ratio (b=500 s/ mm^2) = 1.833 (> 1.234) and lesion to spinal cord ratio (b=1000) = 1.649 (>1.141)

ADC = 1.465 X 10^{-3} mm^2/s (>1.243 X 10^{-3} mm^2/s)

Final diagnosis = Granulomatous inflammation with fungal hyphae (*Aspergillus*)

Case 4:

A 63 years old man with complaints of cough, streaky hemoptysis, fever, loss of appetite for the past 6 months.

Figure 28: Contrast enhanced CT axial section (lung window) showing scattered sub-solid nodules and areas of consolidation predominantly involving the left lower lobe.
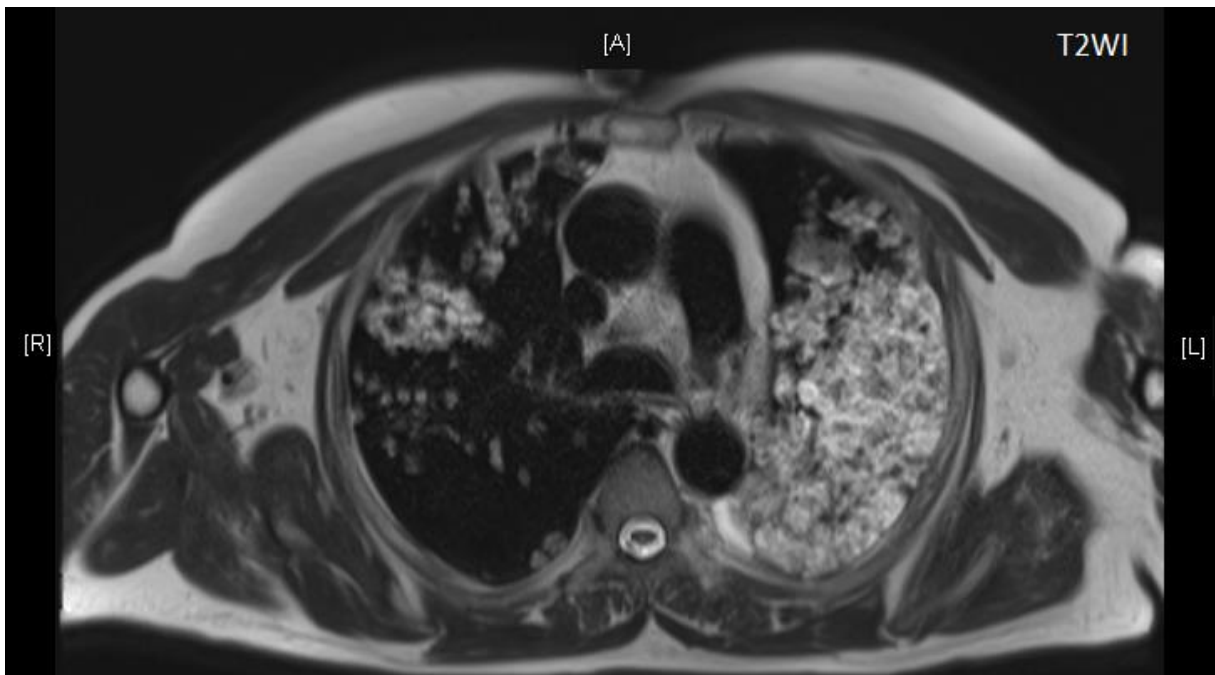
Figure 29: T2W axial sections through the thorax showing T2 hyperintense areas of consolidation predominantly involving the left lower lobe.
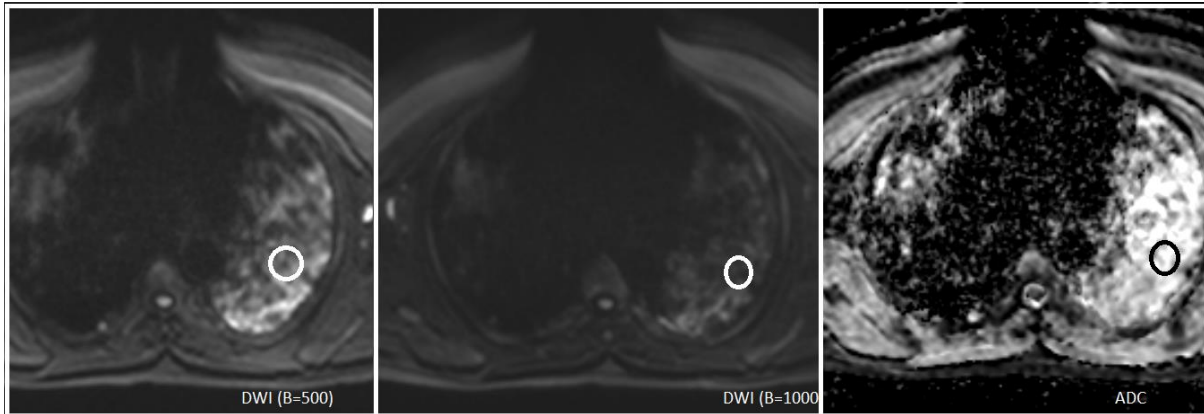
Figure 30: Diffusion weighted images showing T2 shine through effect. The valued derived from the ROIs placed in the areas of consolidation area as shown below.

Lesion to spinal cord ratio (b=500) = 0.622 (< 1.234) and lesion to spinal cord ratio (b=1000) = 0.534 (<1.141)

ADC= 2.041 x 10^{-3} mm^2/s (>1.243 x 10^{-3} mm^2/s)

Final diagnosis = Mucinous adenocarcinoma

(Note: The mucinous type of adenocarcinoma, due to its high intracellular mucin content has a high signal intensity on T2WI with T2 shine though effect on DWI and ADC, hence, unlike other malignancies, has a low LSR and high ADC value)

DISCUSSION

Pulmonary lesions can have various appearances on CT which includes nodule, mass, consolidation and cavity. The disease conditions associated with these CT appearances are many and are as detailed in Table 16.

Table 16: Benign and malignant causes for commonly encountered pulmonary lesions

	Benign	Malignant
Consolidation	Lobar • Infectious - pneumonia • Vascular - contusion, infarction • Others - organizing pneumonia, eosinophilic pneumonia, sarcoidosis Diffuse • Pulmonary edema, ARDS, hypoalbuminemia • Infection – Viral, Pneumocystis jiroveci, bronchopneumonia • Haemorrhage- Wegener's granulomatosis, Henoch Schonlein purpura (HSP) • Others – Acute hypersensitivity pneumonitis, pulmonary alveolar proteinosis etc	• Lung carcinoma with obstructive atelectasis • Adenocarcinoma

Thick walled cavity	• Infection
	  o Pulmonary tuberculosis
	  o Bacterial abscess, cavitating pneumonia
	  o Septic emboli
	  o Other rare infections (coccidiomycosis, actinomycosis etc)
	• Non-infective granulomas
	  o Rheumatoid nodules
	  o Granulomatosis with polyangitis
	• Vascular
		• Primary lung carcinoma (especially squamous cell carcinoma)
		• Cavitating pulmonary metastases (squamous cell carcinoma, adenocarcinoma, sarcoma etc)

	Benign	Malignant
	o Pulmonary infarct	
Nodule or Masses	• Benign granulomas • Inflammatory pseudotumour, sarcoidosis, amyloidosis etc • Intrapulmonary lymph node • Focal scar	• Primary lung malignancy • Pulmonary metastases

In many cases, CECT helps in differentiating benign from malignant lesions based on morphology of the lesion and associated findings. However, in some cases the lesions are indeterminate based on CT features and lesions cannot be characterized as benign or malignant. In such patients, other imaging techniques may help in further characterization. Qualitative or visual assessment of conventional sequences like T1W and T2W images can help determine the cellular characteristics of the lesion to a certain extent. DWI and ADC maps may further help to characterize the lesions at cellular level and could potentially help objectively differentiate between benign and malignant lesions which has major implications on management and prognosis. On DWI, relaxation time on T2 weighted imaging and the corresponding ADC value of that voxel, together determine the signal. Its utility has already been explored and used in the diagnosis of malignancies of other organs like the brain, liver and prostate (62–64). Apparent diffusion coefficient mapping allows quantification of the magnitude of diffusion of water molecules within a tissue (65). The values may be obtained from a region of interest placed within a given slice. Restricted diffusion is indicated by correspondingly lower ADC values and depends on the relative proportion of extracellular to intracellular water content, integrity of the cell membrane, the intracellular organelles and presence of soluble macromolecules in the cytoplasm. The ADC value is found to be low in tissues with high cellular density and those within cells having a higher mitotic index (66). As

a result, malignancies tend to have high signal intensity on diffusion weighted imaging and low ADC value.

Our study assessed the role of diffusion weighted imaging and ADC quantification in diagnosing pulmonary lesions which are indeterminate on CECT. In our study, the signal intensity of the lesion was compared with that of the thoracic skeletal muscle in DWI on a three point scale (hypointense, isointense and hyperintense) and most benign and malignant lesions were found to be hyperintense with no statistically significant difference (p value = 0.590 on b=500 and p value = 0.590 on b=1000). Liu et al (50) who studied 62 patients with 66 pulmonary lesions in a similar three point scale (hypointensity, moderate intensity and hyperintensity) comparing with skeletal muscle found no significant statistical difference between malignant and benign lesions. However they concluded that malignant lesion tends to show hyperintensity and benign lesions tends to show moderate intensity.

A study by Satoh et al (45) which used a 5-point rank scale comparison of lesion to spinal cord signal intensity on DWI with b=1000 for differentiation of malignant and benign pulmonary nodules showed significant difference ($p <0.01$) with 0.796 AUC of ROC and threshold score of 3 with sensitivity of 88.9% and specificity of 79.6%. A few cases of metastatic nodules and adenocarcinoma showed lower scoring and a few granulomas and other inflammatory nodules showed high score in their study. Another study which made a similar comparison on 5 point scale was by Cakir et al (1). They assessed 48 solitary pulmonary nodules of which 30 were malignant and 18 were benign. Their study showed a slightly higher sensitivity and specificity of 93.3% and 88.9% for LSR score of 3 or more.

Our study included quantitative assessment of absolute signal intensity and LSR on DWI with b=500 and b=1000, and ADC quantification. On comparison of mean absolute signal

intensity of the lesions on DWI, malignant lesions showed a higher value on b=500 s/mm^2 and b=1000 s/mm^2 images. Higher b value images of 1000 s/mm^2 which allows higher signal to noise ratio and probably better characterization showed statistically significant difference in mean absolute signal intensity unlike b= 500 s/mm^2 in our study.

The lesion to spinal cord ratio and ADC quantification are more objective methods. LSR is obtained by dividing the absolute signal intensity of the lesion by that of the spinal cord in that section. In our study there was found to be a significant difference between the means of LSR on DWI b=500 (p value=0.002) with a sensitivity of ~ 70% and a specificity of ~ 74.1% for a cut- off value of 1.234 and on b= 1000 (p value= 0.001) with a sensitivity of ~ 70% and a specificity of ~ 85.2% for a cut-off value of ~ 1.141. Higher LSR values indicate higher chances of lesion being malignant. On using ADC value of the solid component to differentiate between benign and malignant lesions, our study showed statistically significant difference (p value= 0.006). Using a cut-off ADC value of 1.248 x 10^{-3} mm^2/s, the sensitivity was 74.1% and specificity was 76.6% with area under the curve of 0.735 in ROC analysis. Lower ADC values indicate higher change of a lesion being malignant. Other studies which made a similar comparison were those by Cakmak et al (68) which studied 47 patients with 62 pulmonary lesions of which 42 were malignant and 20 were benign. Their study showed a sensitivity and specificity of 69% and 85% respectively for LSR cut off value of 0.86 and sensitivity and specificity of 8 6% and 95% respectively for ADC with cut off of 1.78 x 10^{-3} mm^2/s. They assessed minimum ADC value in their study unlike our study where we assessed mean ADC value. Similarly, Uto et al (51) in their study of 28 patients, showed a sensitivity and specificity of 83.3% and 90% respectively for a cut-off LSR value of 1.135 to differentiate benign lesion and lung cancer. They did not find any significant difference in ADC value between lung cancer and benign lesions. They explained that ADC assess pure

diffusion phenomenon whereas signal intensity on DWI is a combined effect of lower diffusion and T2 elongation. In our study, the LSR and ADC quantification showed no significant statistical difference in the diagnostic performance unlike study of Uto et al (51).

Among the 20 cases of malignant lesions, the two outliers were both cases of adenocarcinoma which showed no diffusion restriction with ADC values of 2.041 and 1.799 X 10^{-3} mm^2/s (>95th centile) respectively. In case of mucinous adenocarcinoma, this difference may be accounted for by their distinctive histopathological features. More cellular malignancies have more closely packed cells with a higher nuclear: cytoplasmic ratio. Mucinous adenocarcinoma, however, contains columnar cells (also known as goblet cells) which contain abundant mucin in the intracellular compartment and the cells are arranged in a lepidic pattern giving it the appearance of a consolidation (hence its former name bronchoalveolar carcinoma) and giving it a much higher signal intensity on DWI with no restriction of diffusion. Two cases of squamous cell carcinoma had ADC values above the cut-off in our study, although not as high as mucinous adenocarcinoma.

Among the benign lesions, those that showed an ADC value lower than the cut-off included a few cases benign lesions of tuberculosis (2/11), fungal infection (1/3) and a case of amyloidosis. With respect to the cases of tuberculosis, this was comparable to a study performed by Gupta et al (68) which looked at 70 cases of tuberculomas and tubercular abscesses and found that the cores of the both lesions showed low ADC values with no significant difference between the two groups and they attributed it to the increased cellularity due to its inflammatory response. Similarly in the study by Uto et al, three cases of adenocarcinoma were false negative and one case of organising pneumonia was false positive.

Among the 5 of 20 malignant lesions and 12 of 27 benign lesions that showed necrosis in our study, a higher mean ADC value within the necrotic component was seen in malignant lesions (1.880×10^{-3} mm^2/s) as compared to benign lesions (1.284×10^{-3} mm^2/s). The difference, however was not found to be statistically significant (p value= 0.132). Studies that looked at the role of diffusion weighted imaging in differentiating brain abscesses from necrotic gliobastomas in the brain found that necrotic cores within pyogenic abscesses had lower ADC values than that of necrotic tumours. This was attributed to the fact that the structure of pus itself is, perhaps, responsible for it due to its high cellularity, viscosity and fibrinogen content which severely impairs the mobility of water molecules within (69). The number of cases with necrosis in our study may have been too small to achieve statistical significance.

A meta-analysis of 11 such studies on diffusion weighted imaging of pulmonary lesions (comprising a total of 294 benign and 755 malignant lesions) by Chen et al (70) showed an overall, sensitivity of 82.8% and specificity of 80.1% and concluded that DWI is a fairly accurate non-invasive technique to distinguish between benign and malignant lesions. Another similar meta-analysis done by Shen at al (71) which looked at 31 studies with 2368 pulmonary lesions showed that LSR showed a pooled sensitivity of 80% and specificity of 85% and ADC, a sensitivity of 84% and specificity of 84%. This was higher than the sensitivity and specificity of 70% and 85.2% for LSR (b=1000 s/mm^2) and 80% and 74.1% respectively for ADC, obtained from our study.

Other imaging techniques like PET CT and perfusion studies may help in further characterization of benign versus malignant lesions. Ohno et al (61) studied PET CT versus CT perfusion in 76 pulmonary nodules (43 benign and 27 malignant) and found a sensitivity and specificity of 91% and 52% respectively for a SUV$_{max}$ threshold value of 2 and a

sensitivity and specificity of 86% and 54% respectively for a BV_{PP} threshold value of 2. Although the sensitivity of PET CT is good for identifying malignancy, the specificity is less with false positive results. Many infections, tuberculosis and granulomas may show as false positive on PET CT. Moreover, PET CT is not widely available and involves the use of radioisotopes and contrast media. The specificity of our study was higher with comparable sensitivity than that of PET-CT and dynamic first pass CECT perfusion study by Ohno et al.

The strength of our study, unlike others prior to it lies in its application on lesions that appeared indeterminate on CECT and not those that could be diagnosed as benign or malignant with confidence on CECT. Further DWI is a fast MRI sequence with no need for contrast injection. Our study reveals the added role of DWI in the diagnosis of pulmonary lesions which are indeterminate on CECT of thorax. This is especially relevant in patients with high risk for biopsy.

CONCLUSIONS

- MRI with diffusion weighted imaging is a useful tool for further non-invasive evaluation of pulmonary lesions which are indeterminate on CECT thorax.

- There is a significant difference between benign and malignant pulmonary lesions with regard to

  - Absolute signal intensity on DWI (b=1000 s/mm^2) (p value=0.002)

  - Lesion to spinal cord ratio (LSR) on b=500 s/mm^2 images (cut-off value= 1.234; Sensitivity = 70%; Specificity = 74.1%; AUC = 0.761 and value above the cut-off is suggestive of malignancy)

  - LSR on b=1000 s/mm^2 images (cut-off value= 1.141; Sensitivity = 70%; Specificity = 85.2%; AUC = 0.765 and value above the cut-off is suggestive of malignancy)

- Mean ADC of the solid component (cut-off value=1.248 x 10^3 mm^2/s; Sensitivity=80.1%; Specificity=74.1%; AUC=0.705 and value below the cut-off is suggestive of malignancy.

- If both LSR and ADC are taken together as criteria for malignancy, the sensitivity of diagnosing malignancy is 56 % with specificity of ~96.2%. Instead, if either LSR or ADC is taken alone, the sensitivity of diagnosing malignancy increases to 94%, however, at the expense of a specificity which is reduced to ~63.1%.

- The LSR (b=500 s/mm^2 and 1000 s/mm^2) and ADC quantification of the solid component have similar diagnostic performance for differentiating malignant and benign lesions.

- There was no significant difference found between benign and malignant pulmonary lesions with regard to

- o Absolute signal intensity of lesion on DWI (b=500 s/ mm^2)

- o ADC of the necrotic components of the lesions

- Mucinous adenocarcinoma show very high ADC values above the cut- off value, similar to benign lesions.

- A few cases of benign lesions such as tuberculosis, fungal infection and amyloidosis may show ADC values lower than that of the cut-off value.

- Although histopathological confirmation remains the gold-standard for diagnosis of indeterminate pulmonary lesions, in patients with high risk associated with lung biopsy, a prior knowledge of the likelihood of malignancy based on DWI can help to decide regarding trial antimicrobial therapy or biopsy with increased risk.

- There is a possible selection bias in this study as it conducted in a tertiary care centre with referral of a higher percentage of patients with pulmonary lesions that may not be representative of the general disease distribution.

- The diagnoses of four of our cases were obtained using a combination of clinical data and short term follow up.

- Avoiding susceptibility artefacts on diffusion weighted images in the pulmonary lesion due to air within the lesion and in the surrounding lung parenchyma is a challenge. This could have potentially affected the values obtained from them, lowering the diagnostic performance and area under the ROC curve.

- Number of patients within the subgroups of benign and malignant lesions were insufficient for analysis of statistical significance within the group.

BIBLIOGRAPHY

1. Çakır Ç, Gençhellaç H, Temizöz O, Polat A, Şengül E, Duygulu G. Diffusion Weighted Magnetic Resonance Imaging for the Characterization of Solitary Pulmonary Lesions. Balkan Med J. 2015 Oct;32(4):403–9.

2. Silva CIS, Marchiori E, Souza Júnior AS, Müller NL, Comissão de Imagem da Sociedade Brasileira de Pneumologia e Tisiologia. Illustrated Brazilian consensus of terms and fundamental patterns in chest CT scans. J Bras Pneumol. 2010 Feb;36(1):99–123.

3. Walker CM, Abbott GF, Greene RE, Shepard J-AO, Vummidi D, Digumarthy SR. Imaging pulmonary infection: classic signs and patterns. AJR Am J Roentgenol. 2014 Mar;202(3):479–92.

4. Honda O, Tsubamoto M, Inoue A, Johkoh T, Tomiyama N, Hamada S, et al. Pulmonary cavitary nodules on computed tomography: differentiation of malignancy and benignancy. J Comput Assist Tomogr. 2007 Dec;31(6):943–9.

5. Erasmus JJ, Connolly JE, McAdams HP, Roggli VL. Solitary pulmonary nodules: Part I. Morphologic evaluation for differentiation of benign and malignant lesions. Radiographics. 2000 Feb;20(1):43–58.

6. Shi C-Z, Zhao Q, Luo L-P, He J-X. Size of solitary pulmonary nodule was the risk factor of malignancy. J Thorac Dis. 2014 Jun;6(6):668–76.

7. Henschke CI, Yankelevitz DF, Mirtcheva R, McGuinness G, McCauley D, Miettinen OS, et al. CT screening for lung cancer: frequency and significance of part-solid and nonsolid nodules. AJR Am J Roentgenol. 2002 May;178(5):1053–7.

8. O'donovan PB. The radiologic appearance of lung cancer. Oncology (Williston Park, NY). 1997 Sep;11(9):1387–402; discussion 1402-1404.

9. Jeong YJ, Lee KS, Jeong SY, Chung MJ, Shim SS, Kim H, et al. Solitary pulmonary nodule: characterization with combined wash-in and washout features at dynamic multi-detector row CT. Radiology. 2005 Nov;237(2):675–83.

10. Shim SS, Lee KS, Kim B-T, Choi JY, Chung MJ, Lee EJ. Focal parenchymal lung lesions showing a potential of false-positive and false-negative interpretations on integrated PET/CT. AJR Am J Roentgenol. 2006 Mar;186(3):639–48.

11. Hansell DM, Bankier AA, MacMahon H, McLoud TC, Müller NL, Remy J. Fleischner Society: glossary of terms for thoracic imaging. Radiology. 2008 Mar;246(3):697–722.

12. Franquet T. Imaging of pneumonia: trends and algorithms. European Respiratory Journal. 2001 Jul 1;18(1):196–208.

13. Nachiappan AC, Rahbar K, Shi X, Guy ES, Mortani Barbosa EJ, Shroff GS, et al. Pulmonary Tuberculosis: Role of Radiology in Diagnosis and Management. Radiographics. 2017 Feb;37(1):52–72.

14. Lee Y, Song J-W, Chae EJ, Lee HJ, Lee C-W, Do K-H, et al. CT findings of pulmonary non-tuberculous mycobacterial infection in non-AIDS immunocompromised patients: a case-

controlled comparison with immunocompetent patients. Br J Radiol [Internet]. 2013 Apr [cited 2018 Oct 12];86(1024). Available from: https://www.ncbi.nlm.nih.gov/pmc/articles/PMC3635784/

15. Franquet T. Imaging of pulmonary viral pneumonia. Radiology. 2011 Jul;260(1):18–39.

16. Nemec SF, Eisenberg RL, Bankier AA. Noninfectious inflammatory lung disease: imaging considerations and clues to differential diagnosis. AJR Am J Roentgenol. 2013 Aug;201(2):278–94.

17. Chung MP, Yi CA, Lee HY, Han J, Lee KS. Imaging of Pulmonary Vasculitis. Radiology. 2010 May;255(2):322–41.

18. Sweidan AJ, Singh NK, Stein A, Tanios M. Nodular Sarcoidosis Masquerading as Cancer. Clin Med Insights Circ Respir Pulm Med [Internet]. 2017 Apr 12 [cited 2018 Oct 12];11. Available from: https://www.ncbi.nlm.nih.gov/pmc/articles/PMC5392110/

19. Wong MCS, Lao XQ, Ho K-F, Goggins WB, Tse SLA. Incidence and mortality of lung cancer: global trends and association with socioeconomic status. Scientific Reports. 2017 Oct 30;7(1):14300.

20. WHO | World Cancer Report 2014 [Internet]. [cited 2018 Oct 8]. Available from: http://www.who.int/cancer/publications/WRC_2014/en/

21. Kaur H, Sehgal IS, Bal A, Gupta N, Behera D, Das A, et al. Evolving epidemiology of lung cancer in India: Reducing non-small cell lung cancer-not otherwise specified and quantifying tobacco smoke exposure are the key. Indian J Cancer. 2017 Mar;54(1):285–90.

22. Yang P, Cerhan JR, Vierkant RA, Olson JE, Vachon CM, Limburg PJ, et al. Adenocarcinoma of the lung is strongly associated with cigarette smoking: further evidence from a prospective study of women. Am J Epidemiol. 2002 Dec 15;156(12):1114–22.

23. Cicenas S, Vencevicius V. Lung cancer in patients with tuberculosis. World J Surg Oncol. 2007 Feb 19;5:22.

24. Doll R, Hill AB. The mortality of doctors in relation to their smoking habits; a preliminary report. Br Med J. 1954 Jun 26;1(4877):1451–5.

25. Khuder SA, Mutgi AB. Effect of smoking cessation on major histologic types of lung cancer. Chest. 2001 Nov;120(5):1577–83.

26. Gilham C, Rake C, Burdett G, Nicholson AG, Davison L, Franchini A, et al. Pleural mesothelioma and lung cancer risks in relation to occupational history and asbestos lung burden. Occup Environ Med. 2016 May;73(5):290–9.

27. Adelstein DJ, Tomashefski JF, Snow NJ, Horrigan TP, Hines JD. Mixed small cell and non-small cell lung cancer. Chest. 1986 May;89(5):699–704.

28. Roggli VL, Vollmer RT, Greenberg SD, McGavran MH, Spjut HJ, Yesner R. Lung cancer heterogeneity: a blinded and randomized study of 100 consecutive cases. Hum Pathol. 1985 Jun;16(6):569–79.

29. Kuhlman JE, Fishman EK, Kuhajda FP, Meziane MM, Khouri NF, Zerhouni EA, et al. Solitary bronchioloalveolar carcinoma: CT criteria. Radiology. 1988 May;167(2):379–82.

30. Schuster MR, Scanlan KA. "CT angiogram sign": establishing the differential diagnosis. Radiology. 1991 Dec;181(3):903.

31. Adler B, Padley S, Miller RR, Müller NL. High-resolution CT of bronchioloalveolar carcinoma. AJR Am J Roentgenol. 1992 Aug;159(2):275–7.

32. Golden R. The effect of bronchostenosis upon the roentgen-ray shadows in carcinoma of the bronchus. American Journal of Roentgenology. 1925;(13):21–30.

33. Kurishima K, Kagohashi K, Miyazaki K, Tamura T, Ohara G, Kawaguchi M, et al. Small cell lung cancer with endobronchial growth: A case report. Oncol Lett. 2013 Aug;6(2):553–5.

34. Kaifi JT, Kayser G, Ruf J, Passlick B. The Diagnosis and Treatment of Bronchopulmonary Carcinoid. Dtsch Arztebl Int. 2015 Jul;112(27–28):479–85.

35. Meisinger QC, Klein JS, Butnor KJ, Gentchos G, Leavitt BJ. CT features of peripheral pulmonary carcinoid tumors. AJR Am J Roentgenol. 2011 Nov;197(5):1073–80.

36. Lewis ER, Caskey CI, Fishman EK. Lymphoma of the lung: CT findings in 31 patients. AJR Am J Roentgenol. 1991 Apr;156(4):711–4.

37. Sagawa M, Tsubono Y, Saito Y, Sato M, Tsuji I, Takahashi S, et al. A case-control study for evaluating the efficacy of mass screening program for lung cancer in Miyagi Prefecture, Japan. Cancer. 2001 Aug 1;92(3):588–94.

38. Nishii K, Ueoka H, Kiura K, Kodani T, Tabata M, Shibayama T, et al. A case-control study of lung cancer screening in Okayama Prefecture, Japan. Lung Cancer. 2001 Dec;34(3):325–32.

39. Nawa T, Nakagawa T, Mizoue T, Kusano S, Chonan T, Hayashihara K, et al. A decrease in lung cancer mortality following the introduction of low-dose chest CT screening in Hitachi, Japan. Lung Cancer. 2012 Dec;78(3):225–8.

40. Geva T. Magnetic resonance imaging: historical perspective. J Cardiovasc Magn Reson. 2006;8(4):573–80.

41. Le Bihan D. Diffusion MRI: what water tells us about the brain. EMBO Mol Med. 2014 May;6(5):569–73.

42. Takahara T, Imai Y, Yamashita T, Yasuda S, Nasu S, Van Cauteren M. Diffusion weighted whole body imaging with background body signal suppression (DWIBS): technical improvement using free breathing, STIR and high resolution 3D display. Radiat Med. 2004 Aug;22(4):275–82.

43. Koh D-M, Collins DJ. Diffusion-weighted MRI in the body: applications and challenges in oncology. AJR Am J Roentgenol. 2007 Jun;188(6):1622–35.

44. Zhang X, Fu Z, Gong G, Wei H, Duan J, Chen Z, et al. Implementation of diffusion-weighted magnetic resonance imaging in target delineation of central lung cancer accompanied with atelectasis in precision radiotherapy. Oncol Lett. 2017 Sep;14(3):2677–82.

45. Satoh S, Kitazume Y, Ohdama S, Kimula Y, Taura S, Endo Y. Can malignant and benign pulmonary nodules be differentiated with diffusion-weighted MRI? AJR Am J Roentgenol. 2008 Aug;191(2):464–70.

46. Lyng H, Haraldseth O, Rofstad EK. Measurement of cell density and necrotic fraction in human melanoma xenografts by diffusion weighted magnetic resonance imaging. Magn Reson Med. 2000 Jun;43(6):828–36.

47. Thoeny HC, Forstner R, De Keyzer F. Genitourinary applications of diffusion-weighted MR imaging in the pelvis. Radiology. 2012 May;263(2):326–42.

48. Caravan I, Ciortea CA, Contis A, Lebovici A. Diagnostic value of apparent diffusion coefficient in differentiating between high-grade gliomas and brain metastases. Acta Radiol. 2018 May;59(5):599–605.

49. Gümüştaş S, Inan N, Akansel G, Ciftçi E, Demirci A, Ozkara SK. Differentiation of malignant and benign lung lesions with diffusion-weighted MR imaging. Radiol Oncol. 2012 Jun;46(2):106–13.

50. Liu, Liu, Yu. Usefulness of Diffusion weighted MR imaging in the evaluation of pulmonary lesions.

51. Uto T, Takehara Y, Nakamura Y, Naito T, Hashimoto D, Inui N, et al. Higher sensitivity and specificity for diffusion-weighted imaging of malignant lung lesions without apparent diffusion coefficient quantification 1. Radiology. 2009;252(1):247–254.

52. Gümüştaş S, İnan N, Sarisoy HT, Anik Y, Arslan A, Çiftçi E, et al. Malignant versus benign mediastinal lesions: quantitative assessment with diffusion weighted MR imaging. Eur Radiol. 2011 Nov 1;21(11):2255–60.

53. Mori T, Nomori H, Ikeda K, Kawanaka K, Shiraishi S, Katahira K, et al. Diffusion-Weighted Magnetic Resonance Imaging for Diagnosing Malignant Pulmonary Nodules/Masses: Comparison with Positron Emission Tomography. Journal of Thoracic Oncology. 2008 Apr 1;3(4):358–64.

54. Kanauchi N, Oizumi H, Honma T, Kato H, Endo M, Suzuki J, et al. Role of diffusion-weighted magnetic resonance imaging for predicting of tumor invasiveness for clinical stage IA non-small cell lung cancer. Eur J Cardiothorac Surg. 2009 Apr;35(4):706–10; discussion 710-711.

55. Karaman A, Durur-Subasi I, Alper F, Durur-Karakaya A, Subasi M, Akgun M. Is it better to include necrosis in apparent diffusion coefficient (ADC) measurements? The necrosis/wall ADC ratio to differentiate malignant and benign necrotic lung lesions: Preliminary results. J Magn Reson Imaging. 2017 Oct;46(4):1001–6.

56. Lally BE, Urbanic JJ, Blackstock AW, Miller AA, Perry MC. Small cell lung cancer: have we made any progress over the last 25 years? Oncologist. 2007 Sep;12(9):1096–104.

57. Purandare NC, Rangarajan V. Imaging of lung cancer: Implications on staging and management. Indian J Radiol Imaging. 2015;25(2):109–20.

58. Ofiara LM, Navasakulpong A, Ezer N, Gonzalez AV. The importance of a satisfactory biopsy for the diagnosis of lung cancer in the era of personalized treatment. Curr Oncol. 2012 Jun;19(Suppl 1):S16–23.

59.   Zhang H, Berezov A, Wang Q, Zhang G, Drebin J, Murali R, et al. ErbB receptors: from oncogenes to targeted cancer therapies. J Clin Invest. 2007 Aug;117(8):2051–8.

60.   Matoba M, Tonami H, Kondou T, Yokota H, Higashi K, Toga H, et al. Lung carcinoma: diffusion-weighted mr imaging--preliminary evaluation with apparent diffusion coefficient. Radiology. 2007 May;243(2):570–7.

61.   Ohno Y, Koyama H, Matsumoto K, Onishi Y, Takenaka D, Fujisawa Y, et al. Differentiation of Malignant and Benign Pulmonary Nodules with Quantitative First-Pass 320–Detector Row Perfusion CT versus FDG PET/CT. Radiology. 2011 Feb 1;258(2):599–609.

62.   Diagnostic value of apparent diffusion coefficient in differentiating between high-grade gliomas and brain metastases. - PubMed - NCBI [Internet]. [cited 2017 Oct 22]. Available from: https://www.ncbi.nlm.nih.gov/pubmed/28835111

63.   Hepatocellular Carcinoma and Diffusion-Weighted MRI: Detection and Evaluation of Treatment Response [Internet]. [cited 2018 Sep 19]. Available from: http://www.jcancer.org/v07p1565.htm

64.   Diffusion-Weighted MRI at 3 T for the Evaluation of Prostate Cancer : American Journal of Roentgenology : Vol. 194, No. 6 (AJR) [Internet]. [cited 2018 Sep 19]. Available from: https://www.ajronline.org/doi/full/10.2214/AJR.09.3654

65.   Sener RN. Diffusion MRI: apparent diffusion coefficient (ADC) values in the normal brain and a classification of brain disorders based on ADC values. Comput Med Imaging Graph. 2001 Aug;25(4):299–326.

66.   White NS, McDonald C, Farid N, Kuperman J, Karow D, Schenker-Ahmed NM, et al. Diffusion-weighted imaging in cancer: Physical foundations and applications of Restriction Spectrum Imaging. Cancer Res. 2014 Sep 1;74(17):4638–52.

67.   Wang J, Takashima S, Takayama F, Kawakami S, Saito A, Matsushita T, et al. Head and neck lesions: characterization with diffusion-weighted echo-planar MR imaging. Radiology. 2001 Sep;220(3):621–30.

68.   Gupta RK, Prakash M, Mishra AM, Husain M, Prasad KN, Husain N. Role of diffusion weighted imaging in differentiation of intracranial tuberculoma and tuberculous abscess from cysticercus granulomas-a report of more than 100 lesions. Eur J Radiol. 2005 Sep;55(3):384–92.

69.   Ebisu T, Tanaka C, Umeda M, Kitamura M, Naruse S, Higuchi T, et al. Discrimination of brain abscess from necrotic or cystic tumors by diffusion-weighted echo planar imaging. Magn Reson Imaging. 1996;14(9):1113–6.

70.   Chen L, Zhang J, Bao J, Zhang L, Hu X, Xia Y, et al. Meta-analysis of diffusion-weighted MRI in the differential diagnosis of lung lesions. Journal of Magnetic Resonance Imaging. 2013 Jun 1;37(6):1351–8.

71.   Shen G, Ma H, Liu B, Ren P, Kuang A. Diagnostic Performance of DWI With Multiple Parameters for Assessment and Characterization of Pulmonary Lesions: A Meta-Analysis. AJR Am J Roentgenol. 2018 Jan;210(1):58–67.

STUDY TITLE: Role of DWI and ADC quantification in the evaluation of pulmonary lesions which are indeterminate on Contrast Enhanced Computed Tomography

1. Unique ID (S. No.) : □□□

2. Patient name : □□
              First name   middle name   surname

3. CMCH Vellore Hospital number : □□□□□□□□
4. Telephone number: □□□□□□□□□□
5. Age: □□□years
6. Sex: □□□(1-male; 2-female)
7. Referring department:
□□
□ (1-Gen.medicine; 2-Pulm. medicine; 3-Med. oncology; 4-Cardiothoracic Surg.)

8. Biopsy : □□□□(0-not done; 1-done)

9. Biopsy technique:
□□
□□□□□□□□□□□□□□□□□□□□□□□□□□□□□ (0-not applicable; 1-CT guided; 2-bronchoscopic; 3-open; 4-USG guided; 5- others)

10. Histopathology report-
□□
□□□□□□□□□□□□ (0- not applicable; 1-infection; 2-malignancy; 3-indeterminate; 4-others)

11. If histopathology report- 2(malignancy),
Histological type: □□□□□□□□□□□□□□□
(0- not applicable; 1- adenocarcinoma; 2-squamous cell carcinoma; 3- small cell carcinoma ;
4- undifferentiated; 5-other primary tumour; 6- metastasis) ;   For 5, please
specify_____

12. If histopathology report-2, Histological type-1 then EGFR status: □
(0- not applicable; 1- positive; 7-negative)

13. Sputum cytology: □□ (0- not performed ; 1- positive; 7-negative)

14. Pleural aspirate cytology : □ (0-not performed; 1-positive; 7-negative)

15. Sputum smear : □□ (0- not performed; 1- mycobacterial; 2-other bacterial; 3-fungal; 7-negative);   If other bacterial(2), specify_____

16. Sputum culture: □□ (0- not performed; 1- mycobacterial; 2-other bacterial; 3-fungal; 7-negative);   If other bacterial(2), specify_____

17. MRDWI of lesion compared to thoracic skeletal muscle (b-500): □□□□□□   (1-hypointense; 2-isointense; 3-hyperintense) □

18. MRDWI of lesion compared to thoracic skeletal muscle (b-1000):   □□□□□ (1-hypointense; 2-isointense; 3-hyperintense)
□□
19. Lesion to spinal cord ratio (b-500) -□□□.□□□
20. Lesion to spinal cord ratio (b-1000) -□□□.□□

21. ADC (Apparent diffusion coefficient)- Solid component without necrosis/ air foci -
□□□□□□□□x 10 $^{-3}$ mm/s²

22. Is necrotic component present : □□□(1-yes; 2-no)□□

23. ADC (Apparent diffusion coefficient)-Necrotic component (if present)- □□.□□□□x 10 $^{-3}$ mm/s²

24. Were all lab/ histology test results negative/ inconclusive? □□ (1-yes; 2-no)□□

25. In case of all lab/histology test results being negative/ inconclusive, was resolution/ reduction of lesion on follow up noted? □   (0-not applicable; 1-yes; 2-no)

PATIENT INFORMATION SHEET

Study title:

A study to assess the role of Diffusion weighted magnetic resonance imaging (DWMRI) and Apparent Diffusion Coefficient (ADC) quantification in the evaluation of indeterminate pulmonary lesions

Purpose of the study

The purpose of this study is to use certain non-invasive imaging techniques in MRI to obtain further information regarding the diagnosis of the lung mass detected on CT and compare and correlate it with the final diagnosis which may be obtained through biopsy, blood or sputum tests or on assessment of response to treatment on follow up. If found to be significant, this non-invasive method, although not a substitute for biopsy, could pre-emptively help obtain a working diagnosis for patients who are either unable to or unwilling to undergo the same.

Confidentiality

The participation in the study will remain confidential and shall be known only to the investigators.

Withdrawal from the study

Participation in this study is purely voluntary and you can withdraw from the study anytime

without any reason. It will not compromise your treatment in any way. There won't be any

other risks involved in this study. You need not pay any extra money for the test as the cost will be borne by the research fund.

For any queries, kindly contact-

Dr Shweta Singh,

PG Registrar,

Department of Radiology,

CMC Vellore.

Mobile-+919972824127

Detailed information about the Procedure

What is magnetic resonance imaging, Diffusion weighted imaging and ADC quantification?

The magnetic resonance imaging (MRI) machine is a tube with a centre opening that is about three feet wide. A table slides into the central opening and the patient lies on the table. Pictures of the chest are created using a magnetic field, radio waves and computers. No X-rays are used to create the images. The images made by the MRI will allow your doctor to look at the anatomy of the chest and any masses present within the lung. Additionally, diffusion weighted imaging further helps characterize this mass based on the motion of water molecules within the lung tissue and the lung mass and Apparent Diffusion Coefficient mapping helps objectively quantify it to assess whether the mass is likely to be cancerous or not.

What are the benefits and risks of the MRI test?

This test will potentially help your doctor diagnose the cause of the lung lesion detected on CT. There is no added risks of the test and no ionizing radiation or dye is used. If you should

experience any difficulty or discomfort during the test, the technician can be alerted immediately. There is also no added expense for the patient to undergo MRI.

Before the test

- There are no dietary restriction prior to the scan other than those advised to you based on your underlying medical condition
- Take your medications as instructed by your doctor.

The day of the test

• The test takes about 8-9 minutes. Please allow at least 2 to 3 hours from the time you arrive to the time you leave.

• Please arrive at MRI Room 3 or ASHA MRI room 6 as instructed, 30 minutes prior to the scheduled test time.

• You will be asked to change into a hospital gown and remove all jewellery, dentures and hearing aids.

• Before the test starts, you will be asked questions about your medical history. This is to make sure it is safe for you to have an MRI scan. The procedure will also be explained to you.

• You will be moved onto a table that goes into the MRI scanner.

During the test

- The MRI scan will last for ~ 10 minutes
- You will be asked to lie down still on your back within the gantry which will move into the MRI machine

- During the test, you will hear knocking sounds as the machine takes the pictures. We will also prompt you with instructions. For example, we may ask you to hold your breath for 8 to10 seconds at a time.

- It is important for you to stay as still as possible because movements can create glitches in the pictures.

After the test

- You may resume your normal activity unless your doctor tells you differently.

- Take your regular medications as directed unless your doctor tells you differently.

- By the following day, the test results will be sent to the doctor who ordered the test. You will need to contact your doctor to discuss the results of your test.

- You will then be asked to undergo the scheduled blood or sputum tests with or without a lung biopsy of the lesion or will be subjected to follow up to assess the response to treatment with antibiotics or steroids, if administered

- Keep any scheduled follow-up appointments with your primary doctor

WRITTEN INFORMED CONSENT FORM

Study title: Assessment of indeterminate lung lesions using Magnetic Resonance Imaging

(Diffusion weighted imaging and Apparent Diffusion Coefficient)

Study Number:_____

Subject's initials: _____

Subject's name:_____

Date of Birth/ Age:_____

i) I confirm that I have read and understood the information sheet dated_____ for the

above study and have had the opportunity to ask questions [ ]

ii) I understand that my participation is voluntary and that I am free to withdraw at any time,

without any reason, without my medical care being affected.[ ]

iii) I understand that the Sponsor of the clinical trial, the Ethics committee and the regulatory

authorities will not need my permission to look at my health records both in respect of the

current study and any further research that may be conducted in relation to it, even if I

withdraw from the trial. I agree to this access. However, I understand that my identity will

not be revealed in any information released to third parties or published. [ ]

iv) I agree not to restrict the use of any data or results that arise from this study provided such

a use is for scientific purpose(s)

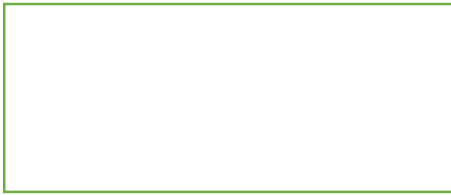v) I agree to take part in the above study. [   ]

Signature/ thumb impression of subject:

Date: _____/____/_____

Signatory's name: _____

Signature:

Or :

Representative:_____

Date: _____/_____/_____

Signatory's name: _____

Signature of the investigator:_____

Date: _____/_____/_____

Study investigator's name: _____

Signature/ thumb impression of the witness: _____

Date: _____/_____/_____

Name and address of the witness:

APPENDIX 3: DATA SHEET

OFFICE OF RESEARCH

INSTITUTIONAL REVIEW BOARD (IRB)

CHRISTIAN MEDICAL COLLEGE, VELLORE, INDIA

Dr. B.J. Prashantham, M.A., M.A., Dr. Min (Clinical)
Director, Christian Counseling Center,
Chairperson, Ethics Committee.

Dr. Anna Benjamin Pulimood, M.B.B.S., MD., Ph.D.,
Chairperson, Research Committee & Principal

Dr. Biju George, M.B.B.S., MD., DM.,
Deputy Chairperson,
Secretary, Ethics Committee, IRB
Additional Vice-Principal (Research)

November 15, 2016

Dr. Shweta Singh,
PG Registrar,
Department of Radiology,
Christian Medical College,
Vellore 632 004.

Sub: **Fluid Research Funding: New Proposal**
Role of Diffusion weighted magnetic resonance imaging and Apparent Diffusion
Coefficient quantification in the evaluation of pulmonary lesions which are indeterminate
on Computed Tomography.
Shweta Singh , Employment Number: 29575, Post Graduate Registrar, Radiology Dr.
Binita Riya Chacko Employment Number: 31893, Radiology,Dr. Aparna Irodi, Emp.
no– 28382, Radiology, Dr. Subin Thomas Kuruvilla, Radiology Dr. Balamugesh,
Pulmonary Medicine, Dr. D. J Christopher , PulmonaryMedicine.

Ref: IRB Min No: 10214 [OBSERVE] dated 08.08.2016

Dear Dr. Shweta Singh,

The Institutional Review Board (Blue, Research and Ethics Committee) of the Christian Medical
College, Vellore, reviewed and discussed your project titled "Role of Diffusion weighted
magnetic resonance imaging and Apparent Diffusion Coefficient quantification in the evaluation
of pulmonary lesions which are indeterminate on Computed Tomography" on August 08th 2016.

The Committee reviewed the following documents:

1. IRB Application format
2. Consent forms and Patient information sheets
3. Cvs of Drs. Binita, Devasahayam, Balamugesh, Aparna, Sridhar G, Subin
   Kuruvilla T, Shweta Singh.
4. No.of documents 1 - 3

The following Institutional Review Board (Blue, Research & Ethics Committee) members were
present at the meeting held on August 08th 2016 in the CREST/SACN Conference Room,
Christian Medical College, Bagayam, Vellore 632002.

2 of 4

Dr. B.J. Prashantham, M.A., M.A., Dr. Min (Clinical)
Director, Christian Counseling Center,
Chairperson, Ethics Committee.

Dr. Anna Benjamin Pulimood, M.B.B.S., MD., Ph.D.,
Chairperson, Research Committee & Principal

Dr. Biju George, M.B.B.S., MD., DM.,
Deputy Chairperson,
Secretary, Ethics Committee, IRB
Additional Vice-Principal (Research)

Name	Qualification	Designation	Affiliation
Dr. Biju George	MBBS, MD, DM	Professor, Haematology, Research), Additional Vice Principal , Deputy Chairperson (Research Committee), Member Secretary (Ethics Committee), IRB, CMC, Vellore	Internal, Clinician
Dr. B. J. Prashantham	MA(Counseling Psychology), MA (Theology), Dr. Min (Clinical Counselling)	Chairperson, Ethics Committee, IRB. Director, Christian Counseling Centre, Vellore	External, Social Scientist
Dr. Anuradha Rose	MBBS, MD, MHSC (Bioethics)	Associate Professor, Community Health, CMC, Vellore	Internal, Clinician
Dr. Jayaprakash Muliyil	BSc, MBBS, MD, MPH, Dr PH (Epid), DMHC	Retired Professor, Vellore	External, Scientist &Epidemiologist
Rev. Joseph Devaraj	BSc, BD	Chaplaincy Department, CMC, Vellore	Internal, Social Scientist
Mr. C. Sampath	BSc, BL	Advocate, Vellore	External, Legal Expert
Dr. Visalakshi. J	MPH, PhD	Lecturer, Biostatistics, CMC, Vellore	Internal, Statistician
Mrs. Sheela Durai	MSc Nursing	Professor, Medical Surgical Nursing, CMC, Vellore	Internal, Nurse
Ms. Grace Rebekha	M.Sc., (Biostatistics)	Lecturer, Biostatistics, CMC, Vellore	Internal, Statistician
Mrs. Pattabiraman	BSc, DSSA	Social Worker, Vellore	External, Lay Person
Dr. Rajesh Kannangai	MD, PhD.	Professor, Clinical Virology, CMC, Vellore	Internal, Clinician
Dr. Balamugesh	MBBS, MD(Int Med), DM, FCCP (USA)	Professor, Pulmonary Medicine, CMC, Vellore	Internal, Clinician

Dr. B.J. Prashantham, M.A., M.A., Dr. Min (Clinical)
Director, Christian Counseling Center,
Chairperson, Ethics Committee.

Dr. Anna Benjamin Pulimood, M.B.B.S., MD., Ph.D.,
Chairperson, Research Committee & Principal

Dr. Biju George, M.B.B.S., MD., DM,
Deputy Chairperson,
Secretary, Ethics Committee, IRB
Additional Vice-Principal (Research)

Dr. Sneha Varkki	MBBS, DCH, DNB	Professor, Paediatrics, CMC, Vellore	Internal, Clinician
Mrs. Emily Daniel	MSc Nursing	Professor, Medical Surgical Nursing, CMC, Vellore	Internal, Nurse
Dr. Sathish	MBBS, MD, DCH	Professor, Child Health, CMC, Vellore	Internal, Clinician
Dr. Inian Samarasam	MS, FRCS, FRACS	Professor, Surgery, CMC, Vellore	Internal, Clinician
Dr. Mathew Joseph	MBBS, MCH	Professor, Neurosurgery, CMC, Vellore	Internal, Clinician
Dr. Ranjith K Moorthy	MBBS, MCh	Professor, Neurological Sciences, CMC, Vellore	Internal, Clinician

We approve the project to be conducted as presented.

Kindly provide the total number of patients enrolled in your study and the total number of withdrawals for the study entitled: "Role of Diffusion weighted magnetic resonance imaging and Apparent Diffusion Coefficient quantification in the evaluation of pulmonary lesions which are indeterminate on Computed Tomography" on a monthly basis. Please send copies of this to the Research Office (research@cmcvellore.ac.in).

Fluid Grant Allocation:

A sum of 1,00,000/- INR (Rupees One Lakh Only) will be granted for 2 years. 50,000/- INR (Rupees Fifty Thousand only) will be granted for 12 months as an 1st Installment. The rest of the 50,000/- INR (Rupees Fifty Thousand only) each will be released at the end of the first year as 2 nd Installment.

Yours sincerely,

Dr. Biju George
Secretary (Ethics Committee)
Institutional Review Board

Dr. BIJU GEORGE
MBBS., MD., DM
SECRETARY - (ETHICS COMMITTEE)
Institutional Review Board,
Christian Medical College, Vellore - 632 002

IRB Min No: 10214 [OBSERVE] dated 08.08.2016

4 of 4